Astrophysical Signatures of Dense Axion Clumps

Ani Prabhu (Stanford University)

10/27/2020

Based on work:

arXiv:2006.10231

arXiv:2005.03700 (with Nicholas Rapidis)

Follow-up work in progress with:

Harikrishnan Ramani (Stanford)

Ryan Janish (Fermilab)

Overview

I. Axions as DM Candidates

II. Formation of Axion Clumps

III. Non-gravitational Lensing Effects of Axion Clumps

IV. Resonant Conversion of Axion Clumps Around NSs.

V. Summary & Conclusions

Overview

I. Axions as DM Candidates

II. Formation of Axion Clumps

III. Non-gravitational Lensing Effects of Axion Clumps

IV. Resonant Conversion of Axion Clumps Around NSs.

V. Summary & Conclusions

Dark Matter Candidates

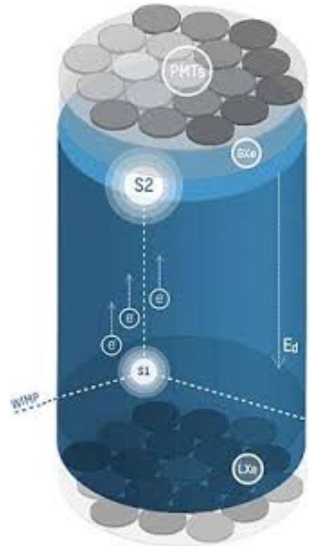

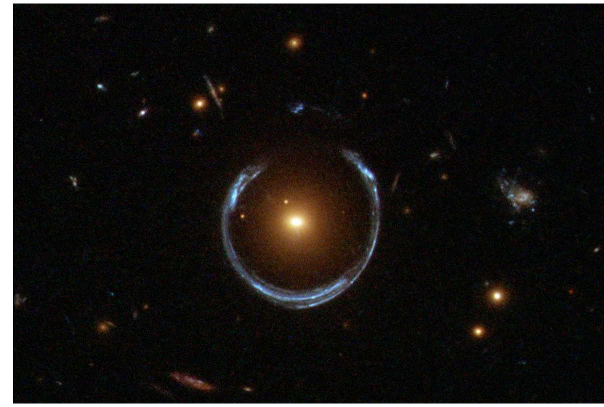

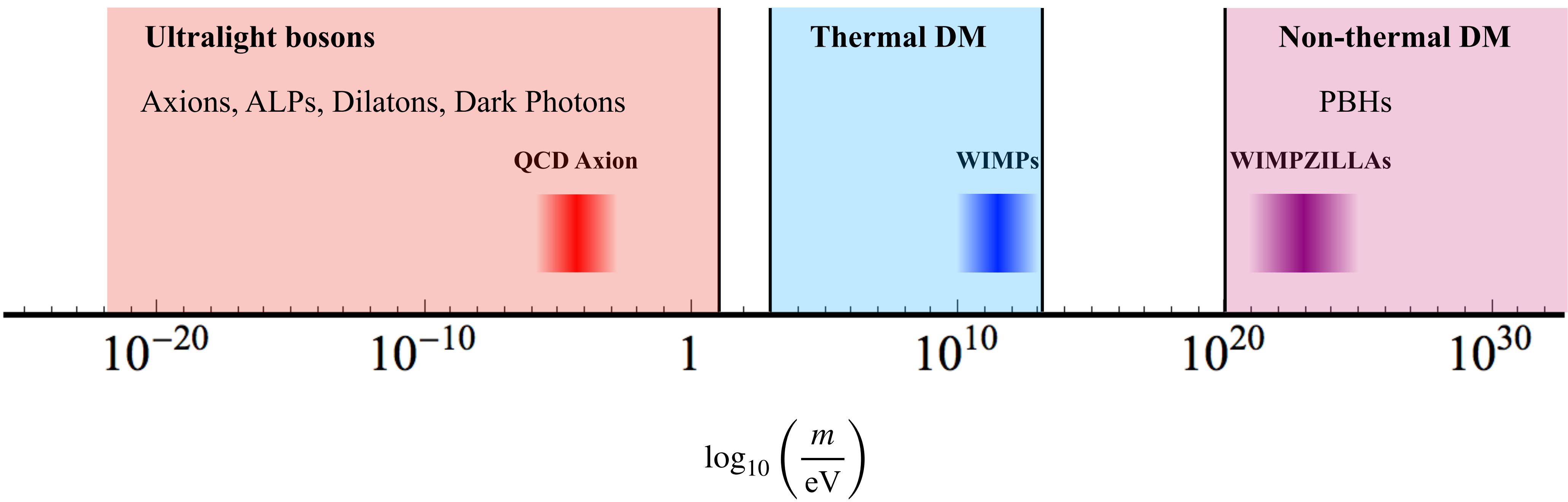

Dark Matter Candidates

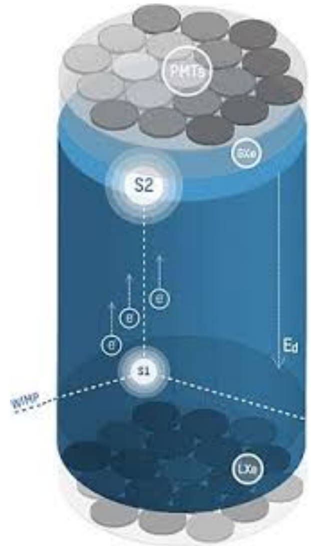

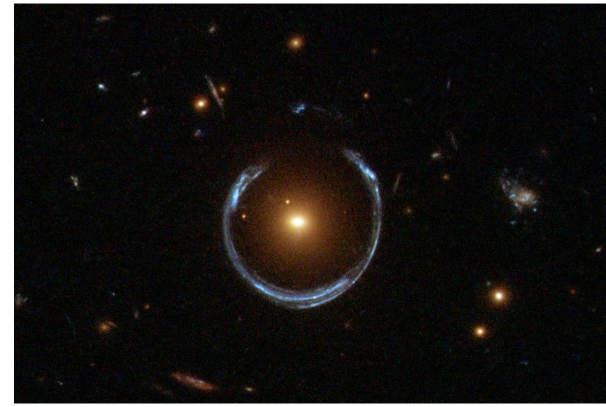

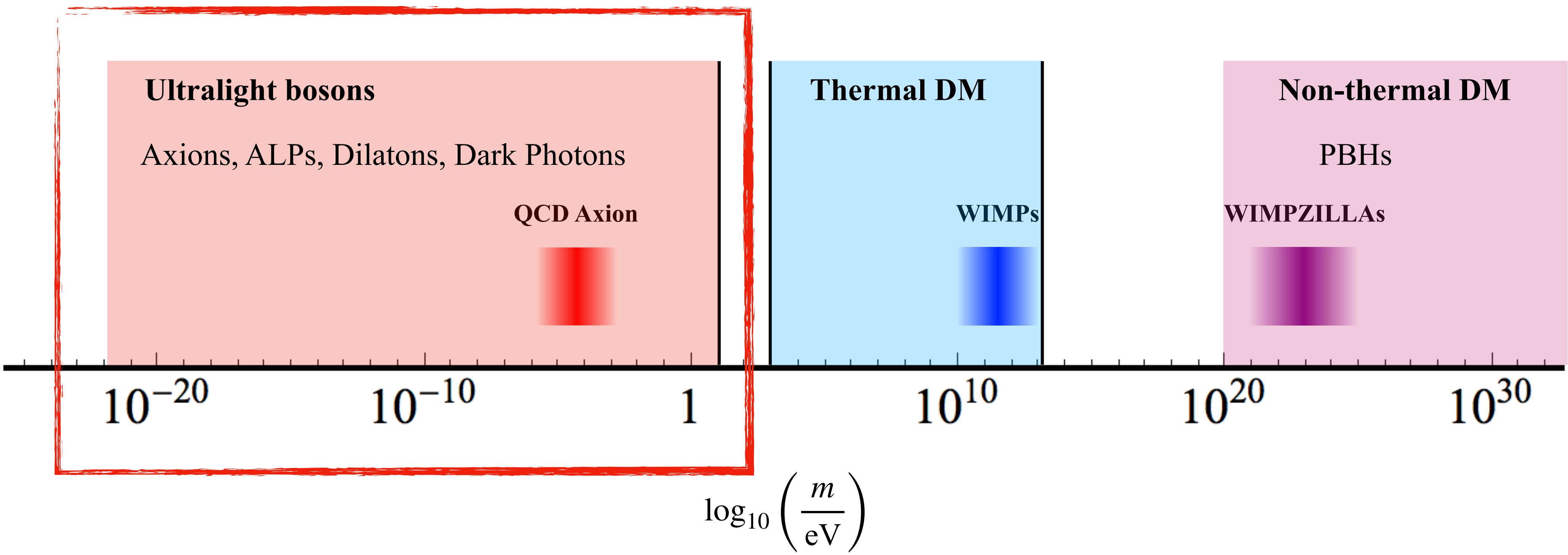

Strong-*CP* Problem & Axions

$$\boxed{\mathscr{L}_{\rm QCD} \supset \frac{\theta}{32\pi^2} \mathrm{Tr}\, G_{\mu\nu}\tilde{G}^{\mu\nu}} \quad \Longrightarrow$$

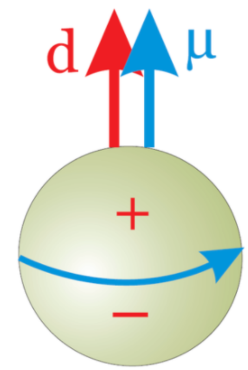

- Upper bound on nEDM $\Longrightarrow$ $\theta_0 + \arg\det M_u M_d \lesssim 10^{-10}$.
- Peccei-Quinn Solution: $\theta \to a(x)/f_a$.
- Instantons generate potential, axion dynamically relaxes to *CP*-conserving value. Vafa & Witten (1984)

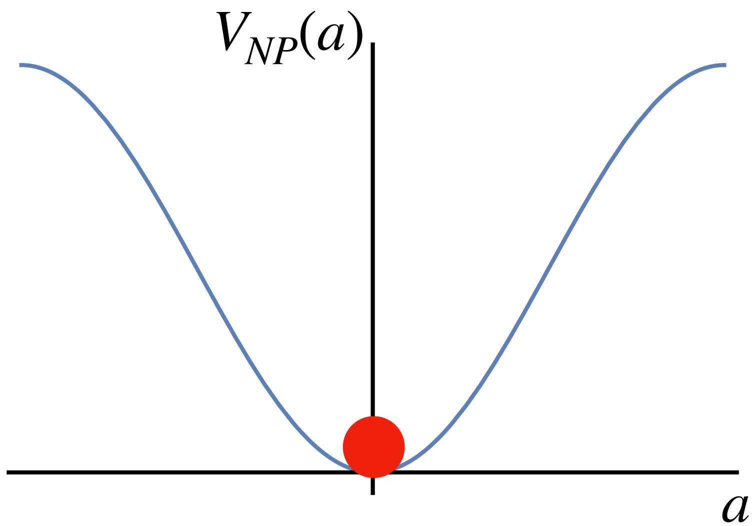

- Ubiquitous in String Theory. Svrček, Witten (2006)

Axions in String Theory

Arvanitaki, Dimopoulos, Dubovsky, Kaloper, March-Russell (2009)

$p-$Forms (A_p)

$+$

Extra Dimensions

$+$

Non-trivial Topology

$\|$

CP-odd scalars (axions)

B_{MN} (NS), C_p(Ramond-Ramond), …

$$M = 0,1,2,3,\underbrace{4,\ldots,D-1}_{\text{Compact Extra Dimensions}}$$

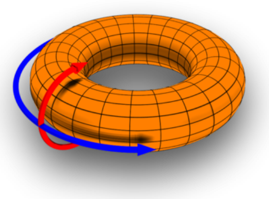

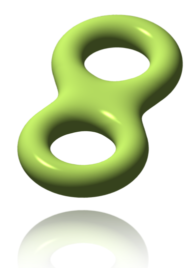

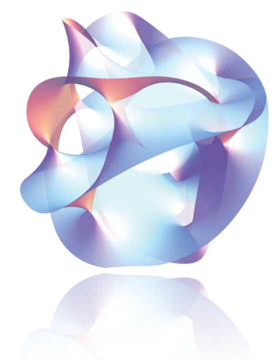

$$A_p = \sum_{i=1}^{b_p} a_i(x)\omega_{p,i}(y)$$

Axions in String Theory

Arvanitaki, Dimopoulos, Dubovsky, Kaloper, March-Russell (2009)

$p-$Forms (A_p)

$+$

Extra Dimensions

$+$

Non-trivial Topology

$||$

CP-odd scalars (axions)

B_{MN} (NS), C_p(Ramond-Ramond), …

$$M = 0,1,2,3,\underbrace{4,\ldots,D-1}_{\text{Compact Extra Dimensions}}$$

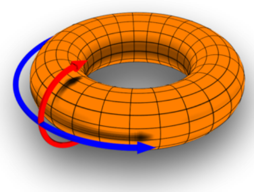

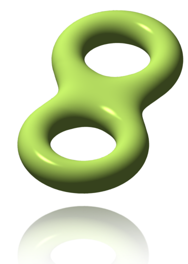

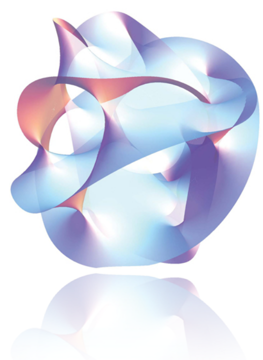

$$A_p = \sum_{i=1}^{b_p} a_i(x)\omega_{p,i}(y)$$

Misalignment Production

$n_{DM}\lambda_a^3 \gg 1$

$(m_a \lesssim 1\ \text{eV})$

Axion: coherently oscillating field

$\phi = \phi_0 \cos(m_a t + \varphi)$

$\ddot{\phi} + 3H\dot{\phi} + m_a^2\phi = 0$

$(\ddot{x} + \gamma\dot{x} + \omega^2 x = 0)$

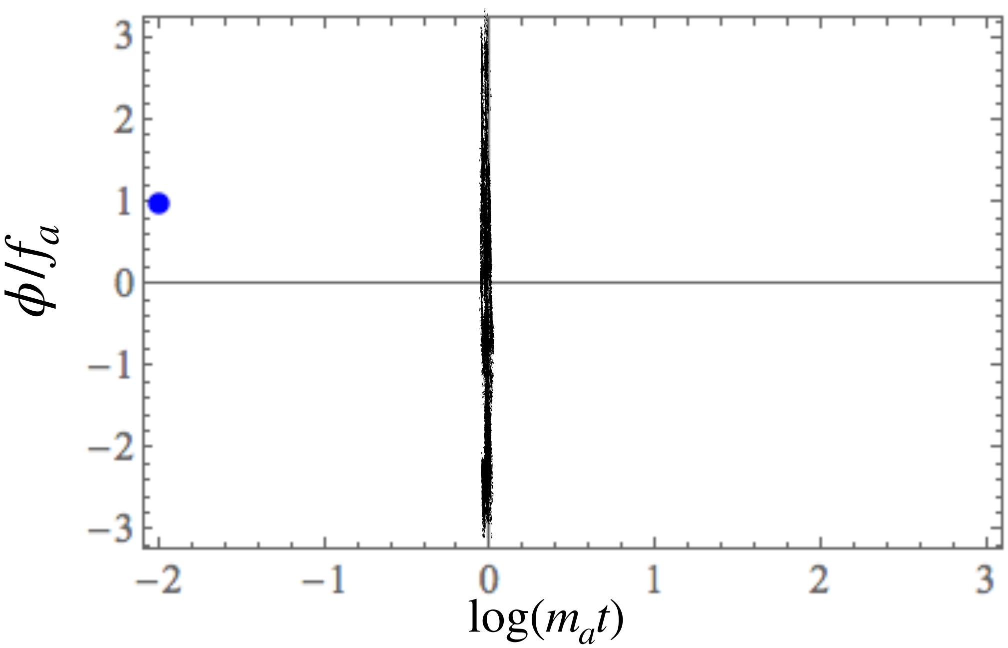

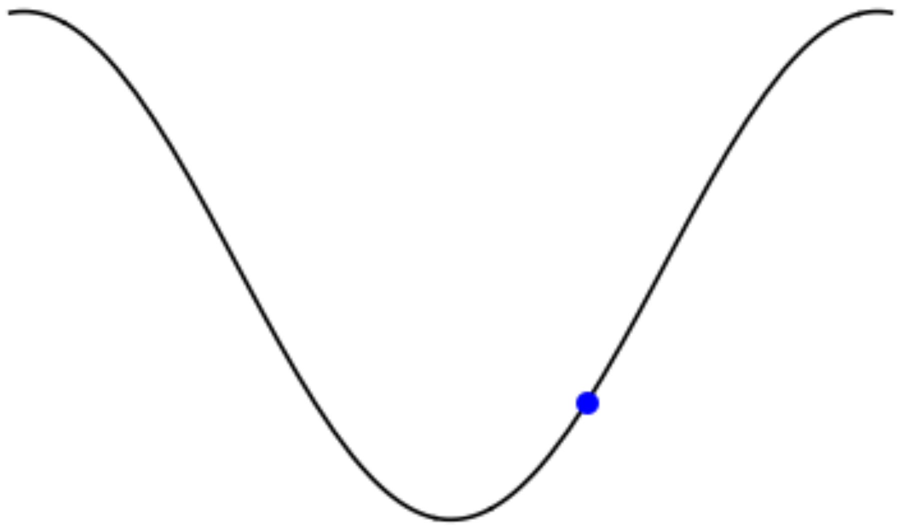

Early time: $\rho_a \propto$ constant

Dark Energy

Late time: $\rho_a \propto a^{-3}$

Dark Matter

Overview

I. Axions as DM Candidates

II. Formation of Axion Clumps

III. Non-gravitational Lensing Effects of Axion Clumps

IV. Resonant Conversion of Axion Clumps Around NSs.

V. Summary & Conclusions

Axion Miniclusters

- Post-inflationary PQ SSB ($f_{PQ} < H_I/2\pi$).
- θ_{PQ} is drawn from $\mathcal{U}[-\pi,\pi]$ in each Hubble volume, uncorrelated across different volumes.
- $\mathcal{O}(1)$ fluctuations on horizon scale at symmetry breaking collapse to form **axion miniclusters (MCs).**

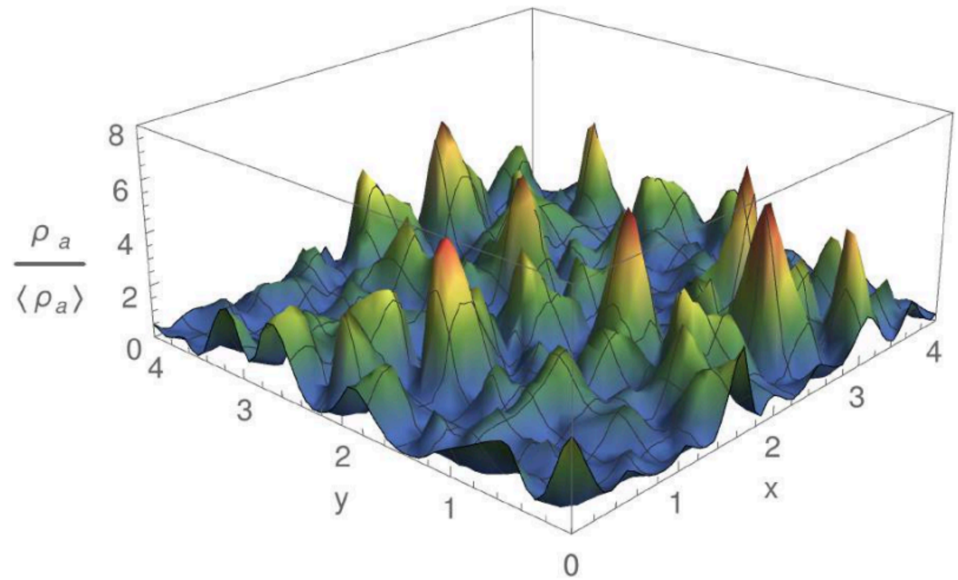

Hardy (2016)

- Present-day abundance of MCs with mass

$$M_{MC} = \frac{4\pi}{3}\left(\frac{\pi}{\mathcal{H}(t_0)}\right)^3 \rho_{0,a} \simeq 2\times 10^{-13}\ M_\odot \left(\frac{m_a}{10^{-6}\ \mathrm{eV}}\right)^{-3/2}$$

$T_{\rm coll} = T_{\rm eq}(1+\Phi)$

$$\rho_{MC} \simeq 7\times 10^6\ \Phi^3(1+\Phi)\ \mathrm{GeV/cm^3} \qquad \bar{\rho}_{CDM} \simeq 0.3\ \mathrm{GeV/cm^3}$$

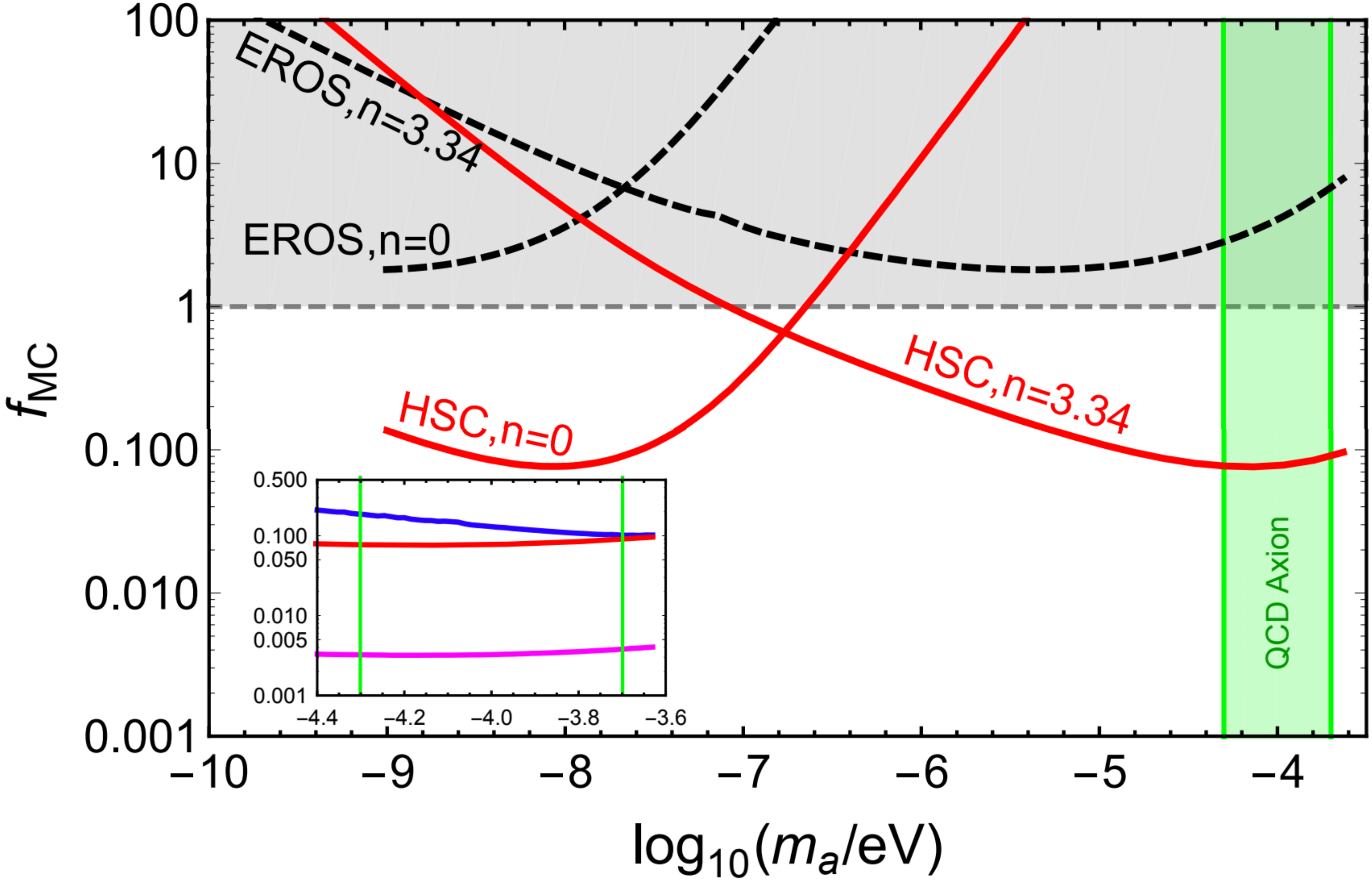

Fairbairn, Marsh, Quevillon & Rozier (2017)

Large Misalignment Mechanism

- At high ϕ_i dynamics probe the full, non-harmonic potential.

$$\ddot{\phi} + 3H\dot{\phi} + V'(\phi) = 0$$

- Delay in the onset of oscillations.

Arvanitaki et al (2019)

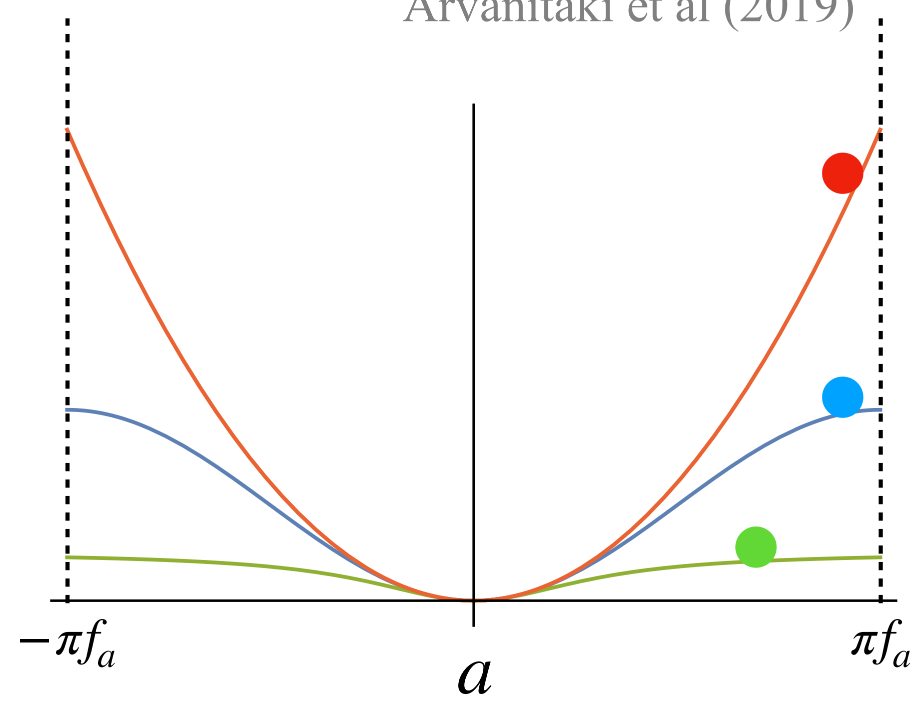

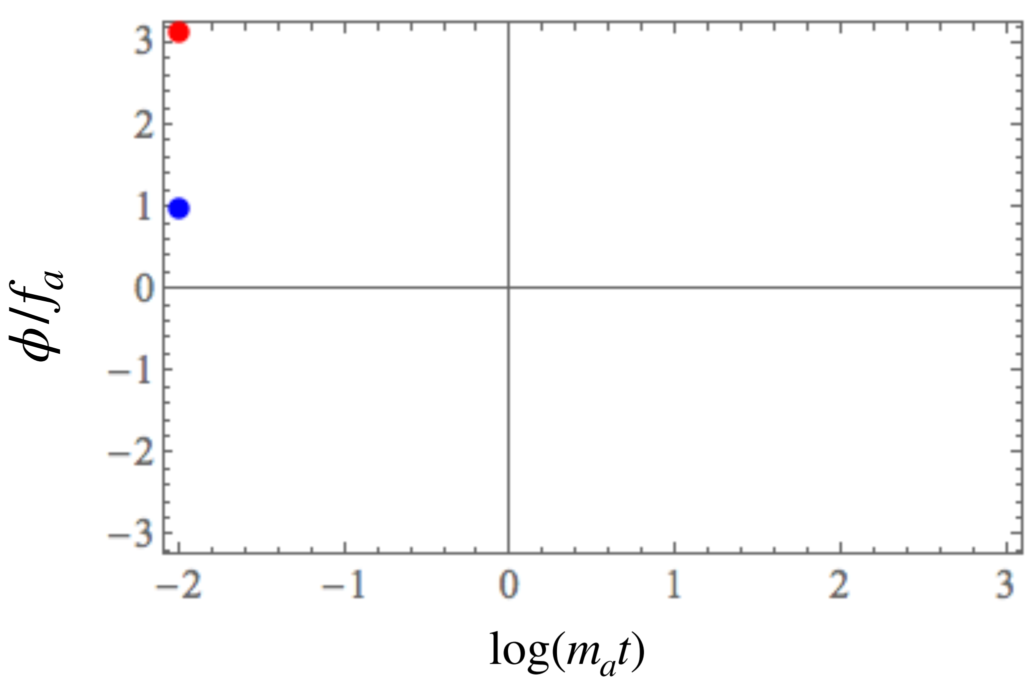

Parametric resonant growth of modes with wavelength $\lambda \sim 2\pi/m_a$ at time oscillations begin.

$$M \simeq 5 \times 10^{-15}\, M_{\odot} \left(\frac{m_a}{10^{-6}\ \mathrm{eV}}\right)^{-3/2}$$

$$\rho \sim 10^3 - 10^7 \rho_{CDM}$$

Femtohalos

Solitons and Oscillons

- At very high misalignment ($\phi_i/f_a - \pi \ll 1$), collapse may take place deep into RD, giving ultradense structures.
- At small scales, scalar field dynamics become important.

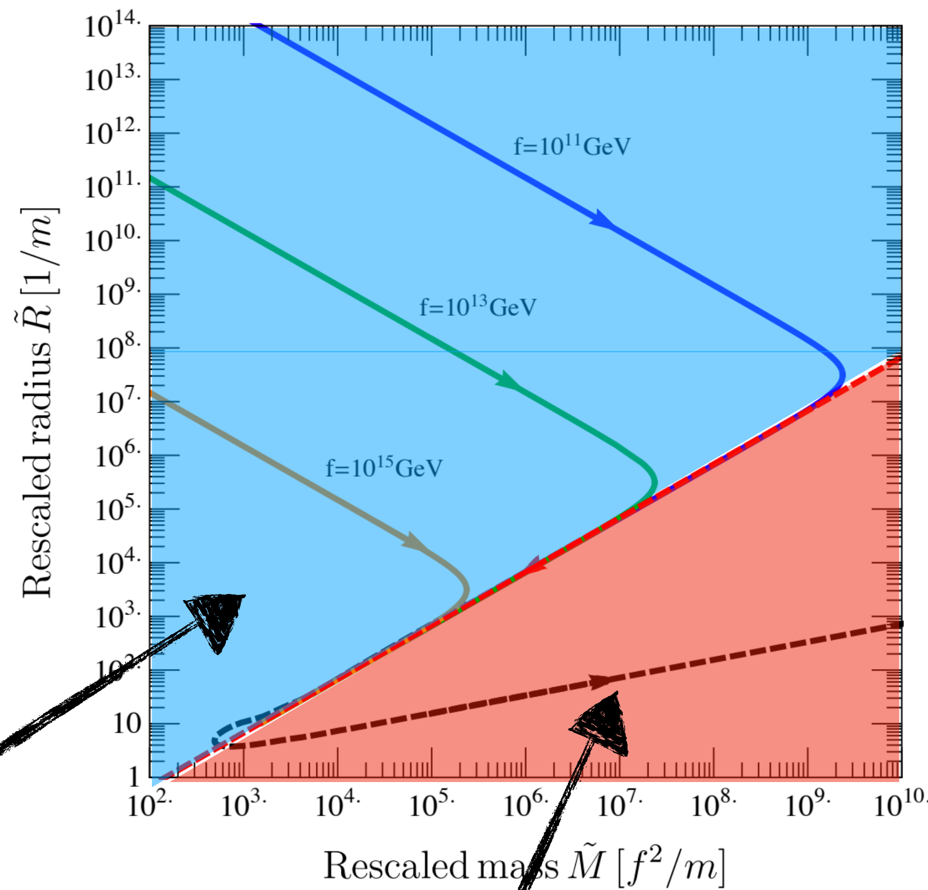

Adapted from Visinelli et al (2017)

Hydrostatic equilibrium of **quantum pressure** + **gravity = solitons**

Hydrostatic equilibrium of **quantum pressure** + **attractive self-interactions = oscillons**

Oscillon Phenomenology

- Central axion amplitude $a_0 \gtrsim f_a$, central density $\rho_0 \sim m_a^2 f_a^2$.
- **Metastable,** QCD axion lifetime $\tau_{QCD} \lesssim 10^3/m_a$, decay before matter-radiation equality.

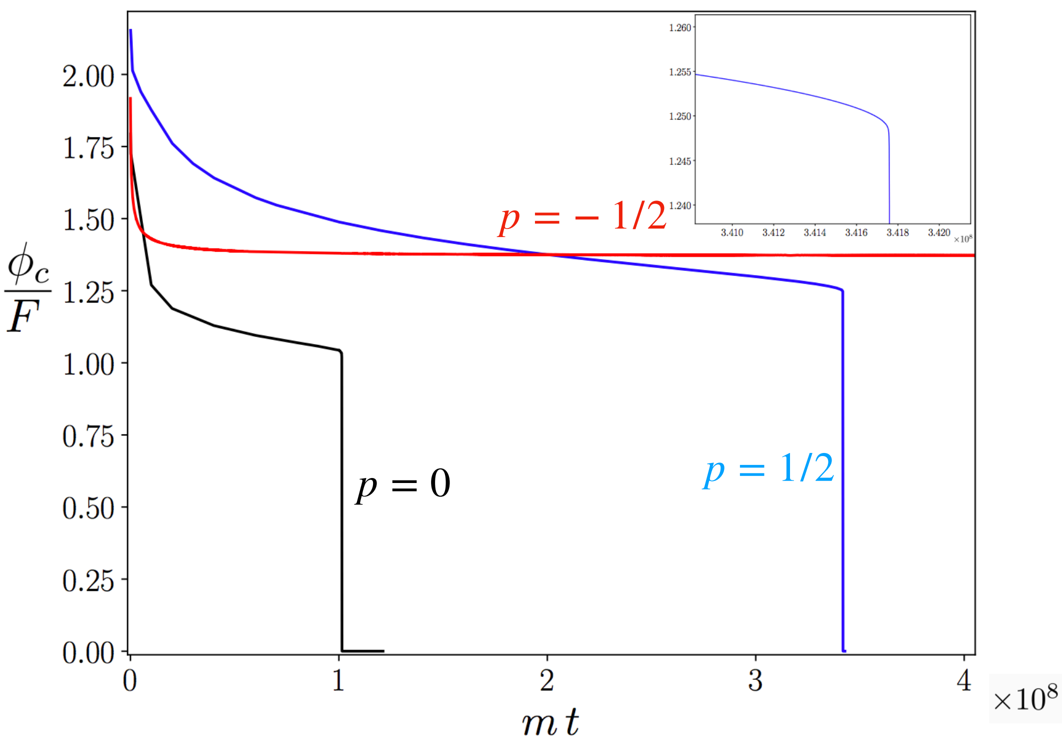

Ollé, Pujolàs & Rompineve (2019)

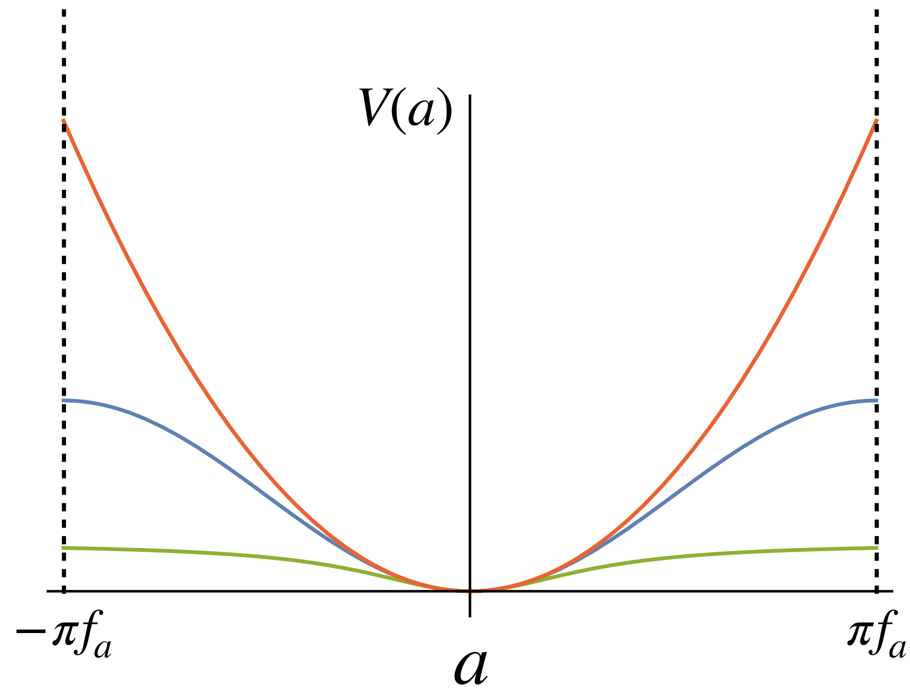

$$V(a) = \frac{1}{2} m_a^2 a^2$$

$$V(a) = m_a^2 f_a^2 \left[1 - \cos\left(\frac{a}{f_a}\right) \right]$$

$$V(a) = \frac{m_a^2 f_a^2}{2p} \left[\left(1 + \frac{a^2}{f_a^2}\right)^p - 1 \right]$$

Summary of Axion Clumps

$m_a = 10^{-6}$ eV, $f_a = 10^{12}$ GeV

Density

Clump	Mass	Density
CDM Halo	$\sim 10^{12}\ M_\odot$	$0.3\ \mathrm{GeV/cm^3}$
Femtohalo	$\sim 5 \times 10^{-15}\ M_\odot$	$(10^3 - 10^7)\ \bar{\rho}_{CDM}$
Minicluster	$\sim 2 \times 10^{-13}\ M_\odot$	$(10^8 - 10^{12})\ \bar{\rho}_{CDM}$
Soliton	$\lesssim 6 \times 10^{-11}\ M_\odot$	$\lesssim 10^{29}\ \bar{\rho}_{CDM}$
Oscillon	$\sim 10^{-15}\ M_\odot$	$\sim 10^{36}\ \bar{\rho}_{CDM}$

Non-Gravitational Signatures of Axion Clumps

$$\mathscr{L} \supset -\frac{g_{a\gamma\gamma}}{4} a\tilde{F}^{\mu\nu}F_{\mu\nu} = -g_{a\gamma\gamma} a\mathbf{E}\cdot\mathbf{B}$$

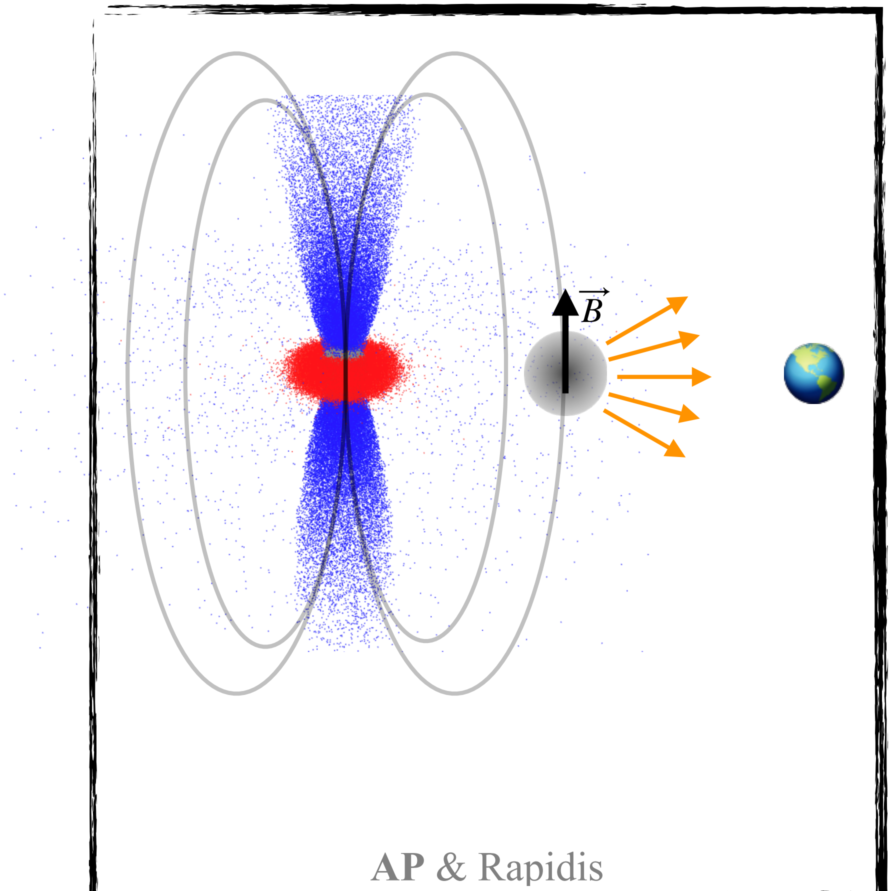

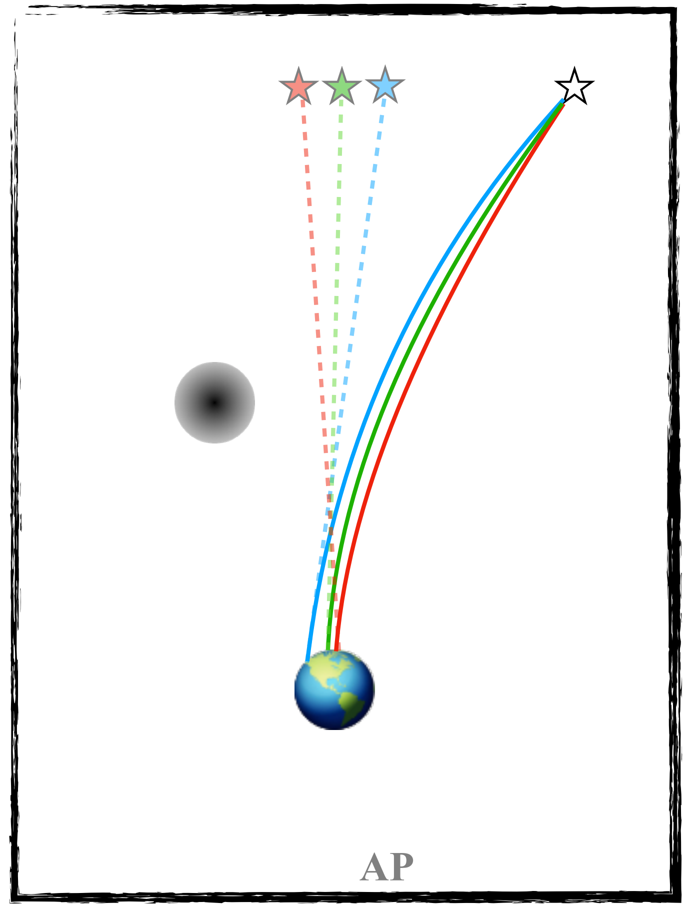

Overview

I. Axions as DM Candidates

II. Formation of Axion Clumps

III. Non-gravitational Lensing Effects of Axion Clumps

IV. Resonant Conversion of Axion Clumps Around NSs.

V. Summary & Conclusions

Axion Electrodynamics

$$\nabla \cdot \mathbf{E} = 0$$

$$\nabla \times \mathbf{E} = -\frac{\partial \mathbf{B}}{\partial t}$$

$$\nabla \cdot \mathbf{B} = 0$$

$$\nabla \times \mathbf{B} = \frac{\partial \mathbf{E}}{\partial t}$$

Axion Electrodynamics

$$\nabla \cdot \mathbf{E} = -g_{a\gamma\gamma} \nabla a \cdot \mathbf{B}$$

$$\nabla \times \mathbf{E} = -\frac{\partial \mathbf{B}}{\partial t}$$

$$\nabla \cdot \mathbf{B} = 0$$

$$\nabla \times \mathbf{B} = \frac{\partial \mathbf{E}}{\partial t} + g_{a\gamma\gamma} (\dot{a}\mathbf{B} + \nabla a \times \mathbf{E})$$

- Modification to photon dispersion relation: refraction, spectral distortions, group delays, etc.

$$\boxed{\omega(\mathbf{k}, \sigma) = |\mathbf{k}| + \sigma \frac{g_{a\gamma\gamma}}{2} \left[\dot{a} + \hat{\mathbf{k}} \cdot \nabla a\right] + \frac{g_{a\gamma\gamma}^2}{16|\mathbf{k}|} \left[\dot{a}^2 - 2(\nabla a)^2 + (\hat{\mathbf{k}} \cdot \nabla a)^2\right] + \mathcal{O}\left((g_{a\gamma\gamma} a)^3\right)}$$

Axion Electrodynamics

$$\nabla \cdot \mathbf{E} = -g_{a\gamma\gamma} \nabla a \cdot \mathbf{B}$$

$$\nabla \times \mathbf{E} = -\frac{\partial \mathbf{B}}{\partial t}$$

$$\nabla \cdot \mathbf{B} = 0$$

$$\nabla \times \mathbf{B} = \frac{\partial \mathbf{E}}{\partial t} + g_{a\gamma\gamma}\left(\dot{a}\mathbf{B} + \nabla a \times \mathbf{E}\right)$$

- Modification to photon dispersion relation: refraction, spectral distortions, group delays, etc.

$$\boxed{\omega(\mathbf{k}, \sigma) = |\mathbf{k}| + \sigma \frac{g_{a\gamma\gamma}}{2}\left[\dot{a} + \hat{\mathbf{k}} \cdot \nabla a\right] + \frac{g_{a\gamma\gamma}^2}{16|\mathbf{k}|}\left[\dot{a}^2 - 2(\nabla a)^2 + (\hat{\mathbf{k}} \cdot \nabla a)^2\right] + \mathcal{O}\left((g_{a\gamma\gamma} a)^3\right)}$$

Optical Effects at $\mathcal{O}(g_{a\gamma\gamma})$

- Linear-order term is a total derivative and only contributes through boundary terms.

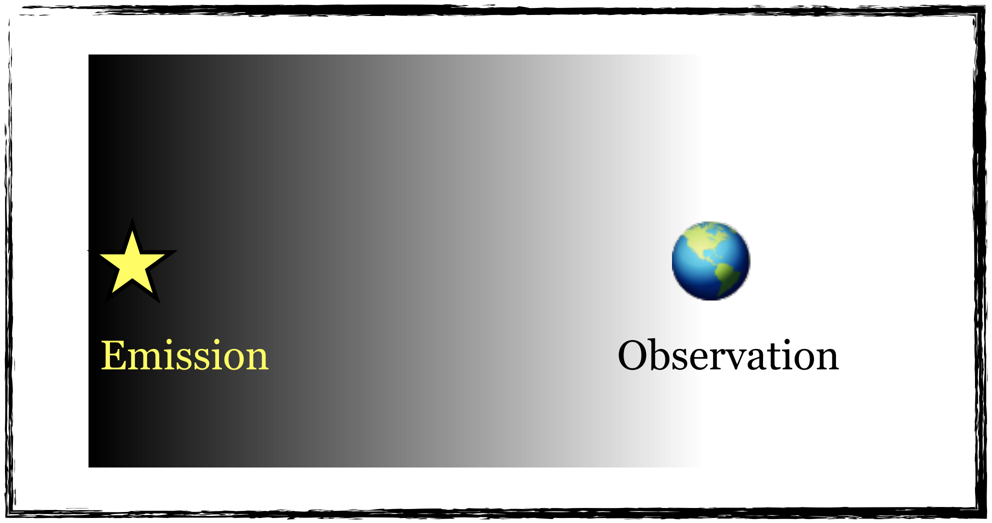

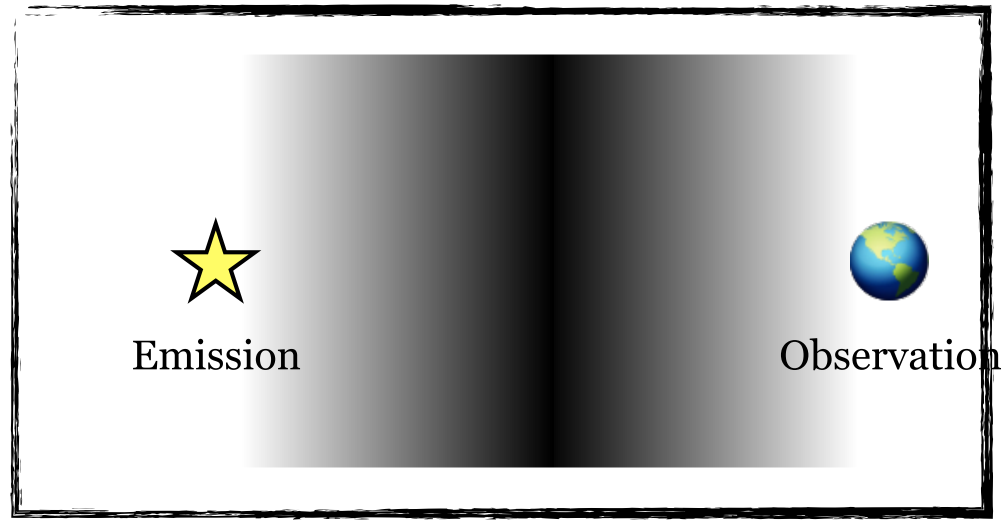

Optical Effects at $\mathcal{O}(g_{a\gamma\gamma})$

- Linear-order term is a total derivative and only contributes through boundary terms.

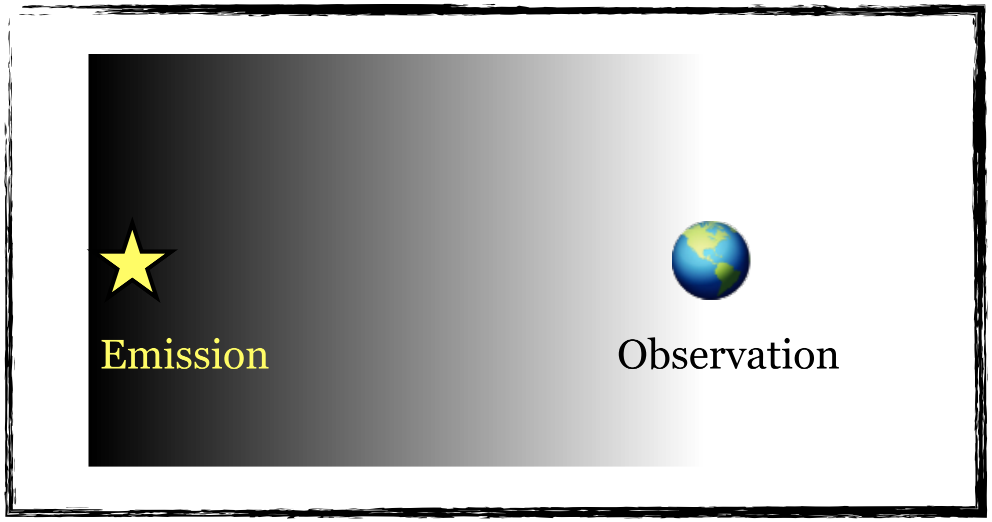

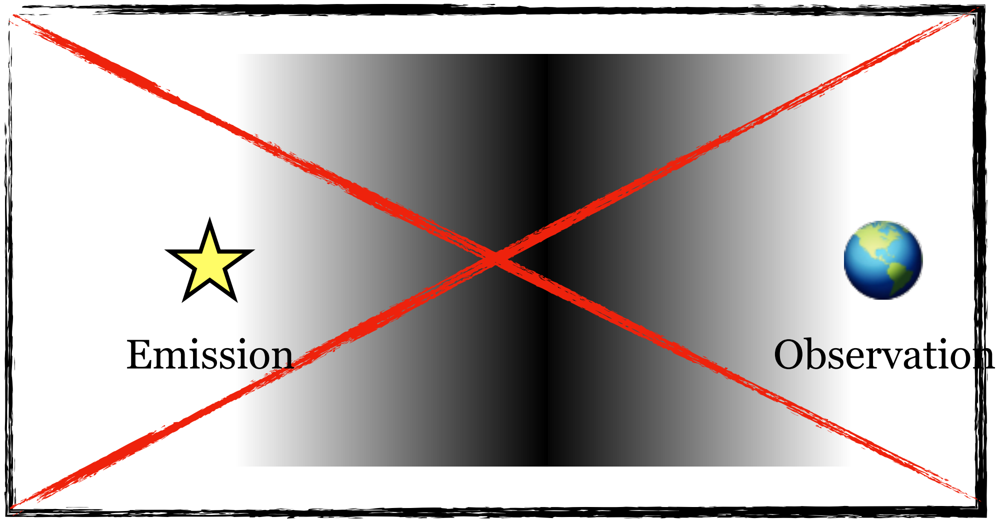

Optical Effects at $\mathcal{O}(g_{a\gamma\gamma})$

- Linear-order term is a total derivative and only contributes through boundary terms.

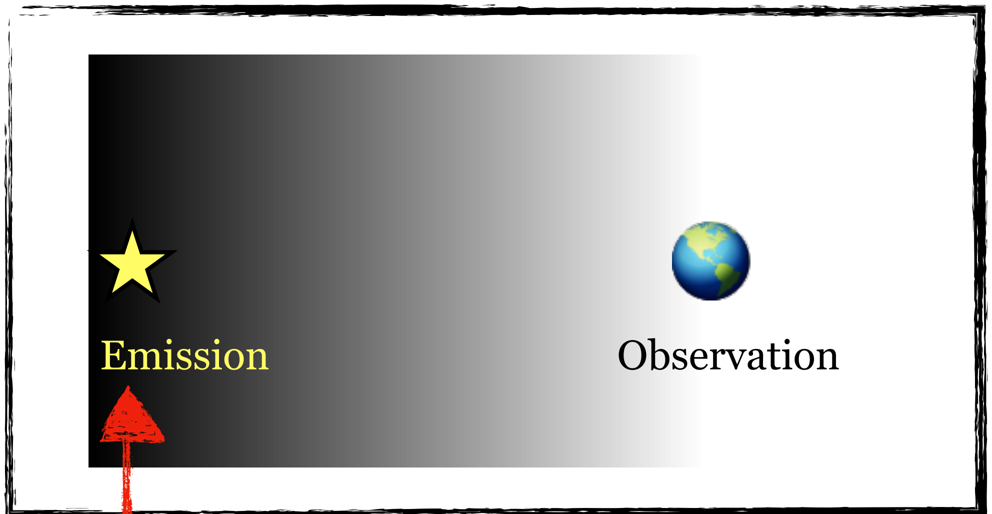

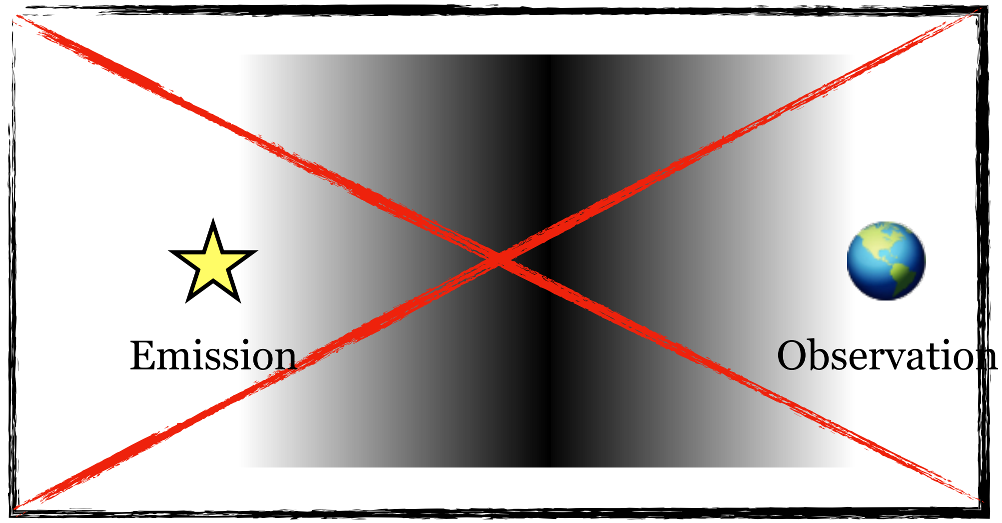

CMB

Relative phase shift between LHCP, RHCP light

$$\boxed{\delta\phi \sim g_{a\gamma\gamma}\left[a(t_{em}, \mathbf{x}_{em}) - a(t_{obs}, \mathbf{x}_{obs})\right]}$$

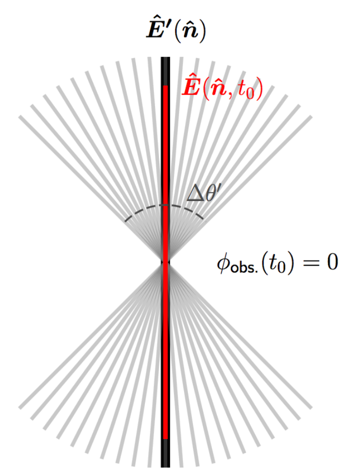

Fedderke, Graham, Rajendran (2019)

Optical Effects at $\mathcal{O}(g_{a\gamma\gamma})$

- Linear-order term is a total derivative and only contributes through boundary terms.

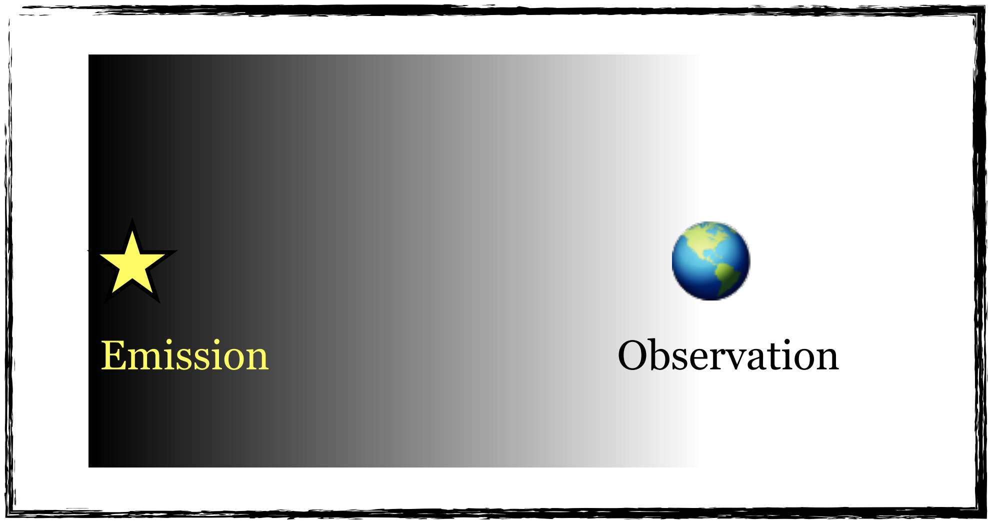

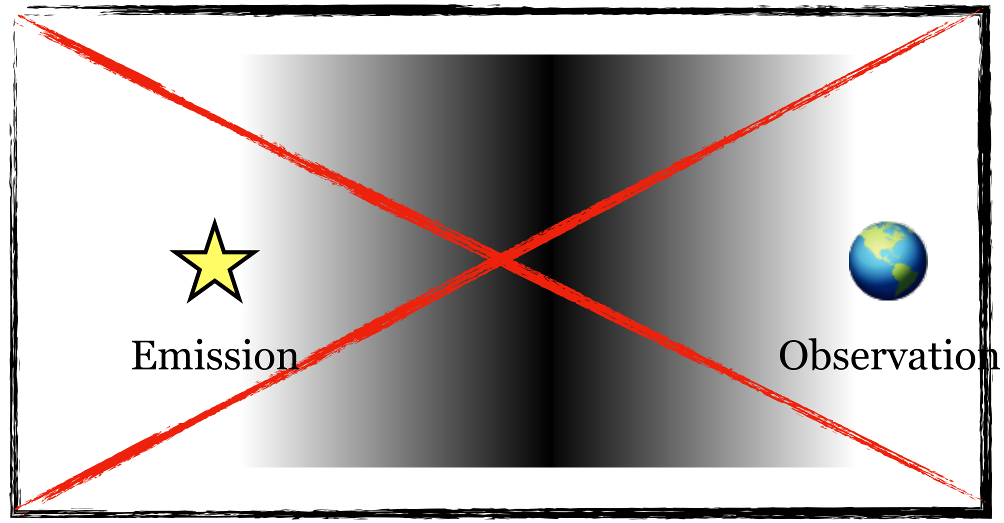

<u>Birefringent refraction</u>

$$\boxed{\frac{\delta \mathbf{k}}{k} \sim g_{a\gamma\gamma}\left[\nabla_\perp a(t_{em}, \mathbf{x}_{em}) - \nabla_\perp a(t_{obs}, \mathbf{x}_{obs})\right]}$$

$\nabla_\perp$: Transverse gradient

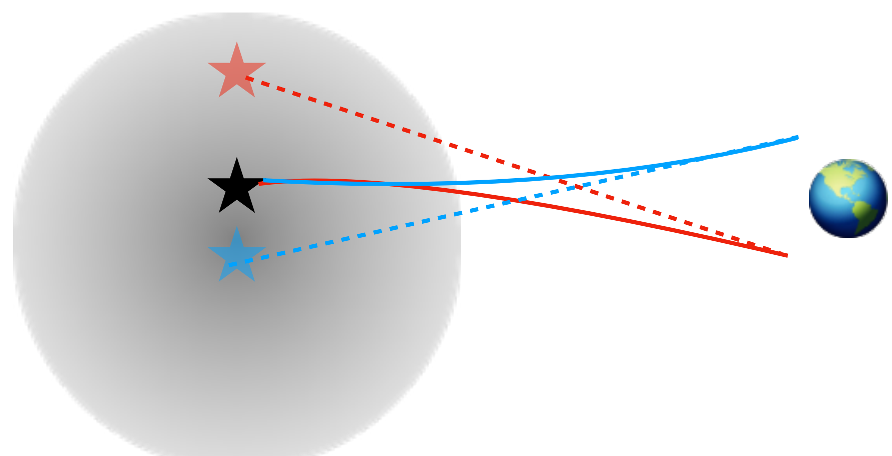

Axion Electrodynamics

$$\nabla \cdot \mathbf{E} = -g_{a\gamma\gamma} \nabla a \cdot \mathbf{B}$$

$$\nabla \times \mathbf{E} = -\frac{\partial \mathbf{B}}{\partial t}$$

$$\nabla \cdot \mathbf{B} = 0$$

$$\nabla \times \mathbf{B} = \frac{\partial \mathbf{E}}{\partial t} + g_{a\gamma\gamma} (\dot{a}\mathbf{B} + \nabla a \times \mathbf{E})$$

- Modification to photon dispersion relation: refraction, spectral distortions, group delays, etc.

$$\boxed{\omega(\mathbf{k}, \sigma) = |\mathbf{k}| + \sigma \frac{g_{a\gamma\gamma}}{2} \left[\dot{a} + \hat{\mathbf{k}} \cdot \nabla a\right] + \frac{g_{a\gamma\gamma}^2}{16|\mathbf{k}|} \left[\dot{a}^2 - 2(\nabla a)^2 + (\hat{\mathbf{k}} \cdot \nabla a)^2\right] + \mathcal{O}\left((g_{a\gamma\gamma} a)^3\right)}$$

Refraction at $\mathcal{O}(g_{a\gamma\gamma}^2)$

- Quadratic order term in dispersion relation gives integrated effects.

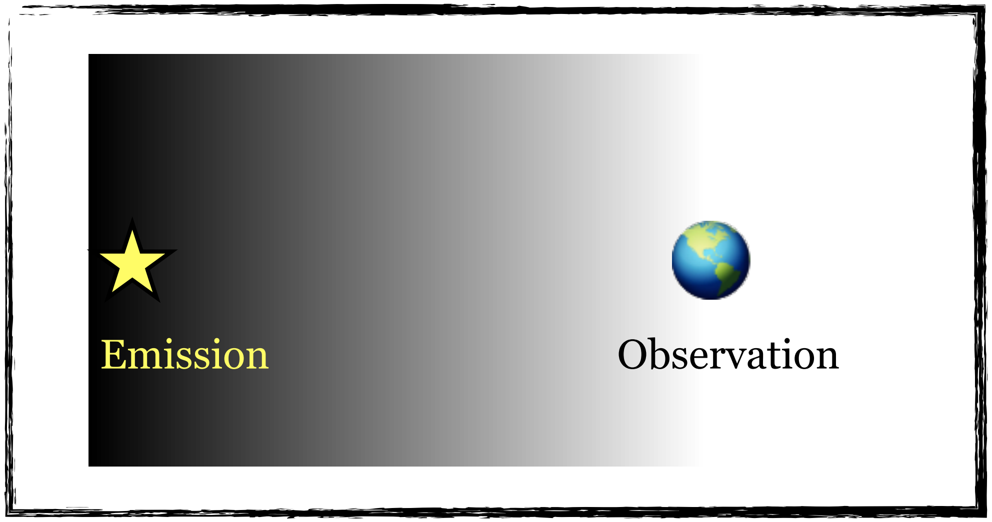

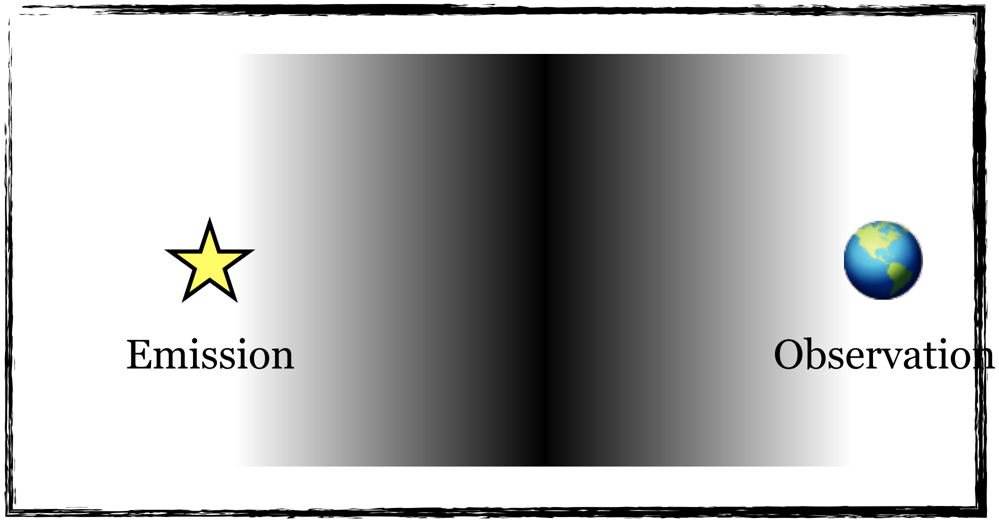

Refraction at $\mathcal{O}(g_{a\gamma\gamma}^2)$

- Quadratic order term in dispersion relation gives integrated effects.

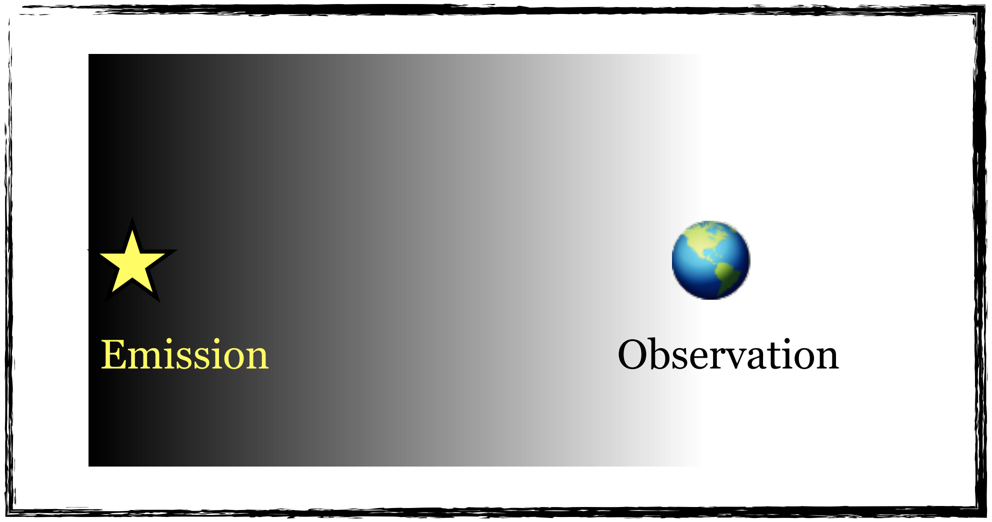

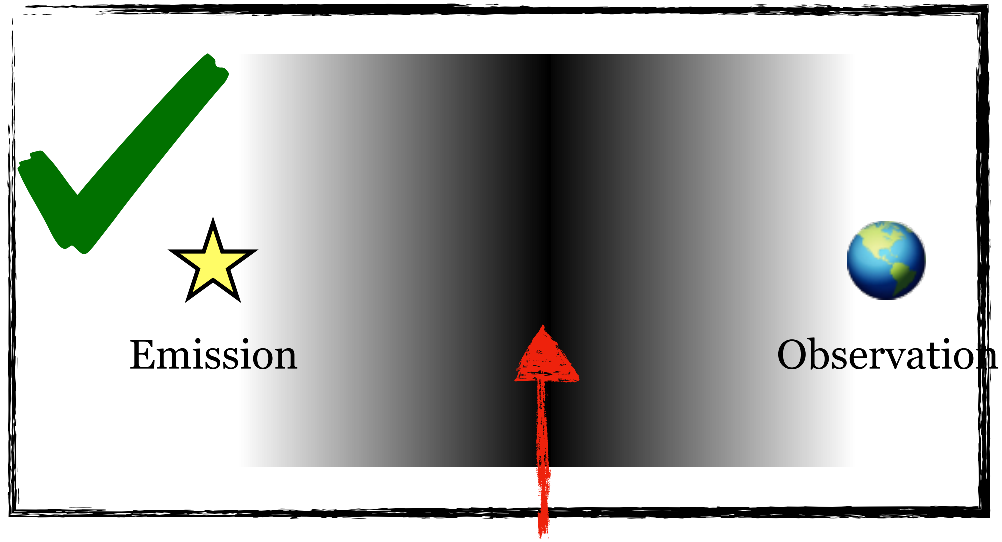

Axions Stars, Halos

<u>Bending Angle</u>

$$\delta\theta = \frac{g_{a\gamma\gamma}^2}{8\,|\mathbf{k}_0|^2}\int_{t_{\text{em}}}^{t_{\text{obs}}} \nabla_\perp \dot{a}^2(t', \mathbf{x}_0(t';\xi))dt'$$

Gaussian Profile

$$\delta\theta \sim \frac{g_{a\gamma\gamma}^2 a_0^2}{|\mathbf{k}_0|^2}\left(\frac{b}{R_a}\right) e^{-b^2/R_a^2}$$

b : Impact parameter

R_a : Axion star radius

a_0 : Central axion density

Refraction at $\mathcal{O}(g^2_{a\gamma\gamma})$

- Quadratic order term in dispersion relation gives integrated effects.

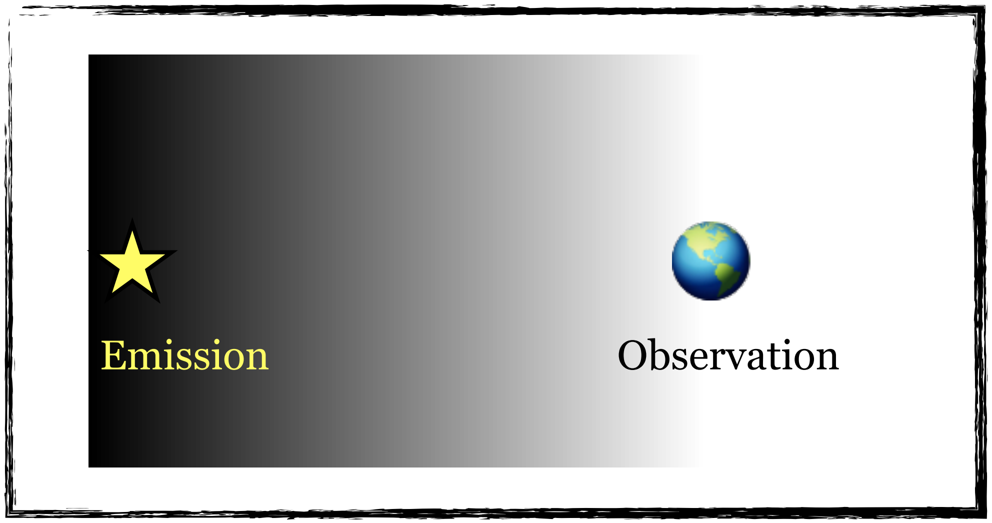

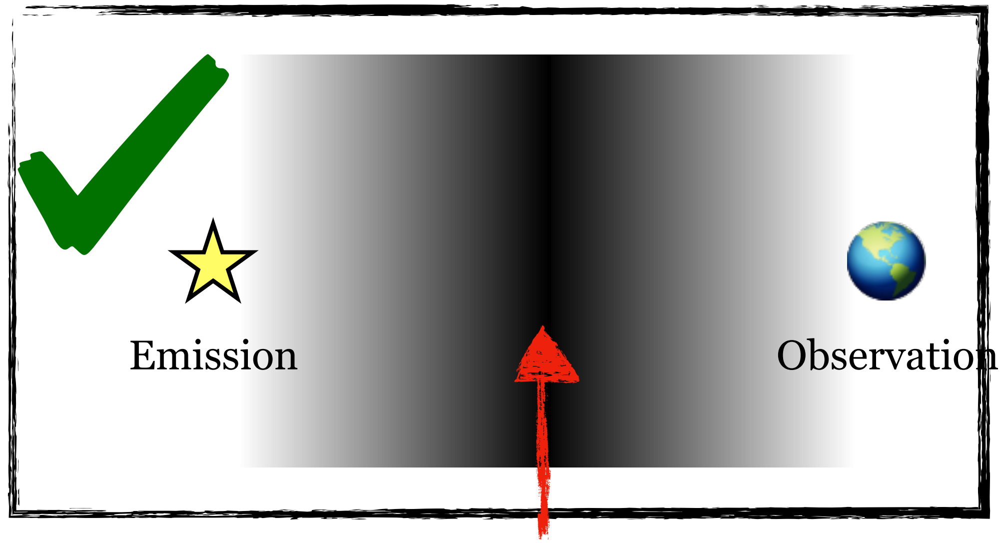

Axions Stars, Halos

<u>Bending Angle</u>

$$\delta\theta = \frac{g^2_{a\gamma\gamma}}{8|\mathbf{k}_0|^2}\int_{t_{\rm em}}^{t_{\rm obs}} \nabla_\perp \dot{a}^2(t', \mathbf{x}_0(t';\xi))dt'$$

Gaussian Profile

$$\delta\theta \sim \frac{g^2_{a\gamma\gamma}a_0^2}{|\mathbf{k}_0|^2}\left(\frac{b}{R_a}\right)e^{-b^2/R_a^2}$$

Effects stronger at low frequency $\Longrightarrow$ **radio** observations

b : Impact parameter

R_a : Axion star radius

a_0 : Central axion density

Lensing Effects: Axions vs. Gravity

Magnitude (Oscillons)

$$\delta\theta_a(b = R_a) \approx 10^{-6}\,\text{rad}\left(\frac{\phi_0}{f_a}\right)^2\left(\frac{m_a}{\omega}\right)^2 \qquad \text{(Axions)}$$

$$\delta\theta_G(b = R_a) \approx 10^{-10}\,\text{rad}\left(\frac{f_a}{10^{12}\,\text{GeV}}\right)^2\left(\frac{m_a R_a}{10}\right)^2 \qquad \text{(Gravity)}$$

Lensing Effects: Axions vs. Gravity

Magnitude (Oscillons) $f_a \lesssim 10^{14}$ GeV

$$\boxed{\delta\theta_a(b = R_a) \approx 10^{-6}\ \mathrm{rad}\left(\frac{\phi_0}{f_a}\right)^2\left(\frac{m_a}{\omega}\right)^2}$$ (Axions)

$$\delta\theta_G(b = R_a) \approx 10^{-10}\ \mathrm{rad}\left(\frac{f_a}{10^{12}\ \mathrm{GeV}}\right)^2\left(\frac{m_a R_a}{10}\right)^2$$ (Gravity)

Lensing Effects: Axions vs. Gravity

Magnitude (Oscillons)

$f_a \lesssim 10^{14}$ GeV

$$\boxed{\delta\theta_a(b = R_a) \approx 10^{-6}\,\text{rad}\left(\frac{\phi_0}{f_a}\right)^2\left(\frac{m_a}{\omega}\right)^2}$$ (Axions)

$$\delta\theta_G(b = R_a) \approx 10^{-10}\,\text{rad}\left(\frac{f_a}{10^{12}\,\text{GeV}}\right)^2\left(\frac{m_a R_a}{10}\right)^2$$ (Gravity)

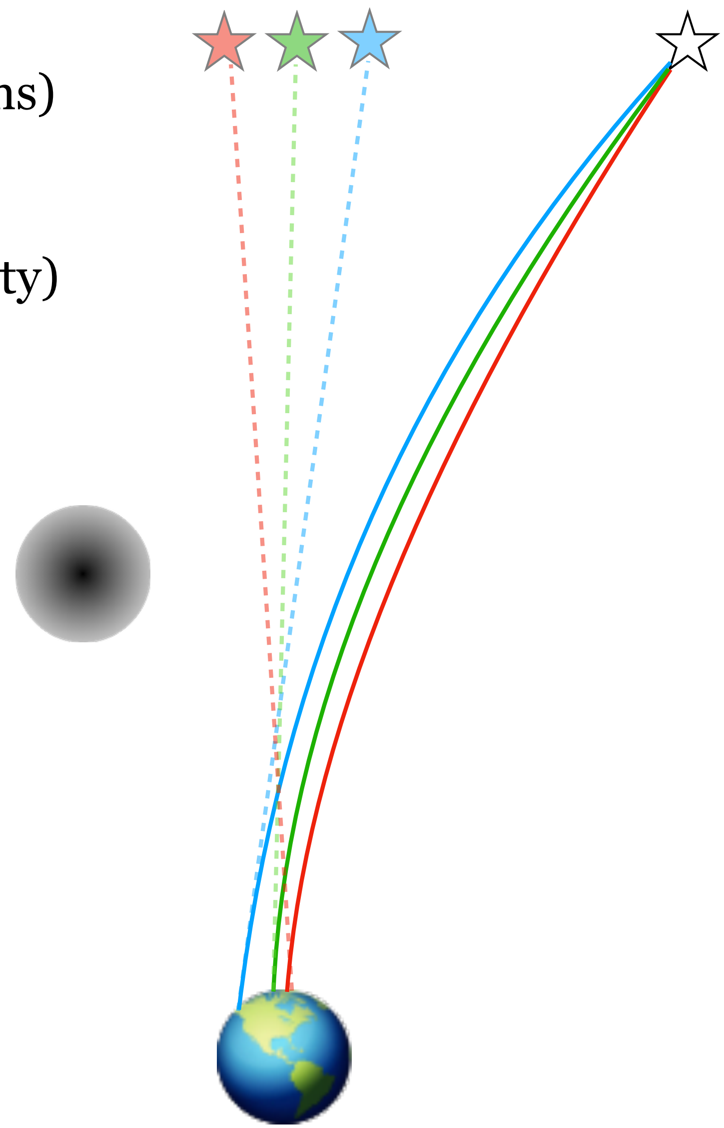

Dispersion

$$\left.\begin{array}{l}\text{Axion: Dispersive}\\ \\ \text{Gravity: Achromatic}\end{array}\right\}$$ Can be differentiated by multi-wavelength observations.

We can search for such lensing signatures with high-precision astrometric missions (SKA).

Observation with SKA

- Lensing of background radio sources by axion stars leads to apparent positional shifts.
- SKA can make astrometric measurements of background radio sources reaching $\sim \mu$as precision.

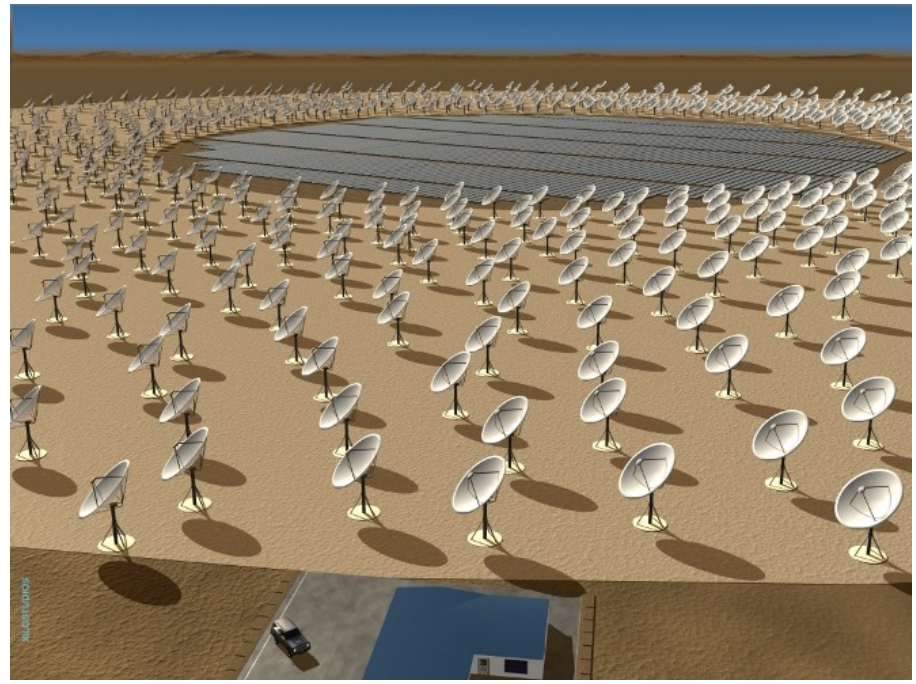

Figure: NAOC

- High-cadence monitoring of background radio source positions can give information about dark matter subhalos.

van Tilburg et al (2018)

Observables

- Candidate signals: close approach between AS and one (mono-blip) or multiple (multi-blip) background radio sources.

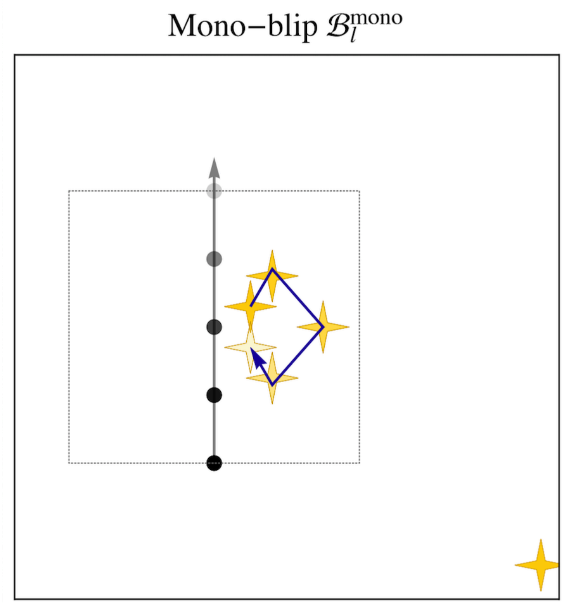

Figure: van Tilburg et al (2018)

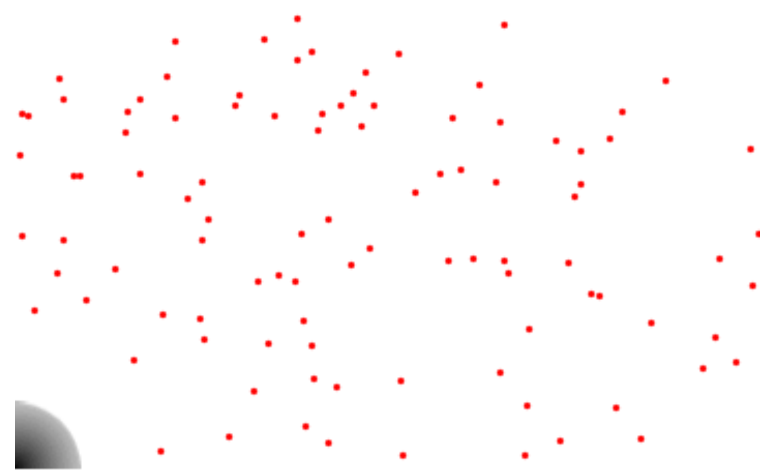

Observables

- Candidate signals: close approach between AS and one (**mono-blip**) or multiple (multi-blip) background radio sources.

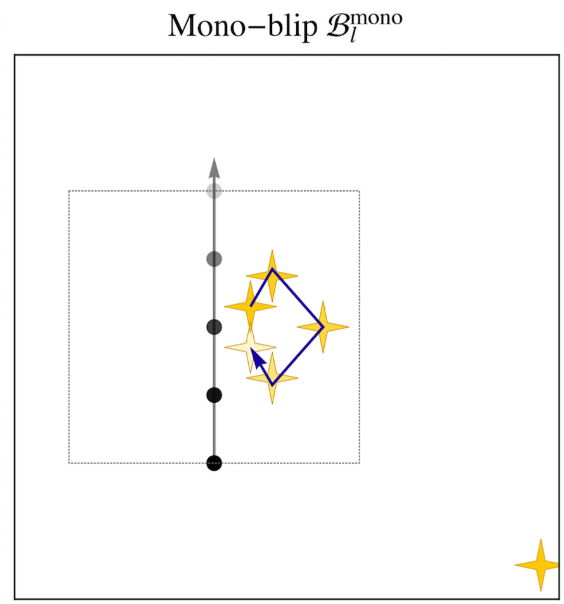

Figure: van Tilburg et al (2018)

<u>Mono-blip Statistic</u>

$$\mathscr{B}_{mono}[\mathbf{x}_\ell(t)] = \frac{1}{\sigma^2_{\delta\theta}} \sum_n \delta\boldsymbol{\theta}_a\left(\mathbf{x}_\ell(t_n)\right) \cdot \Delta\boldsymbol{\theta}(t_n)$$

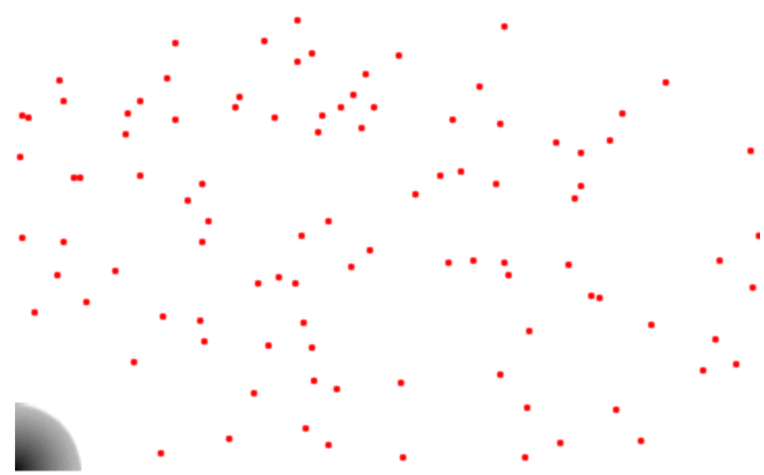

Observables

- Candidate signals: close approach between AS and one (**mono-blip**) or multiple (multi-blip) background radio sources.

<u>Mono-blip Statistic</u>

$$\mathscr{B}_{mono}[\mathbf{x}_\ell(t)] = \frac{1}{\sigma^2_{\delta\theta}} \sum_n \delta\boldsymbol{\theta}_a\left(\mathbf{x}_\ell(t_n)\right) \cdot \Delta\boldsymbol{\theta}(t_n)$$

Lens Path

Angular Position Noise

Axion Lensing

Residuals

- SNR $\propto \left\langle \mathscr{B}[\mathbf{x}_\ell(t)] \right\rangle^{1/2}$.

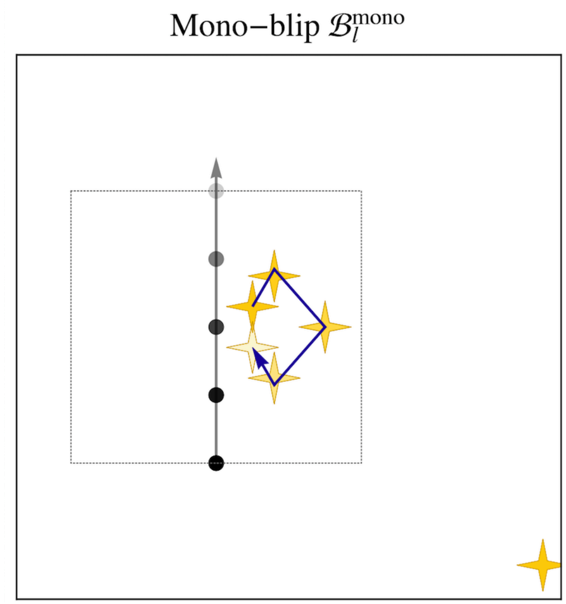

Figure: van Tilburg et al (2018)

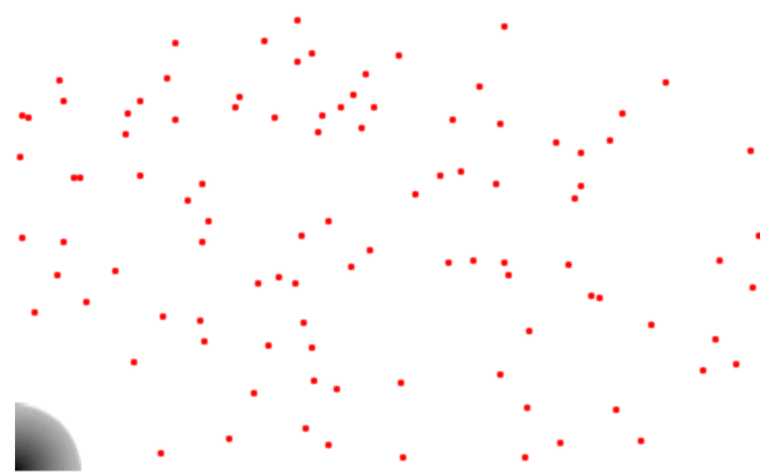

Oscillon Sensitivity

- Daily measurements of 10^8 radio sources with angular precision $\sigma_{\delta\theta} = 10\ \mu$as.

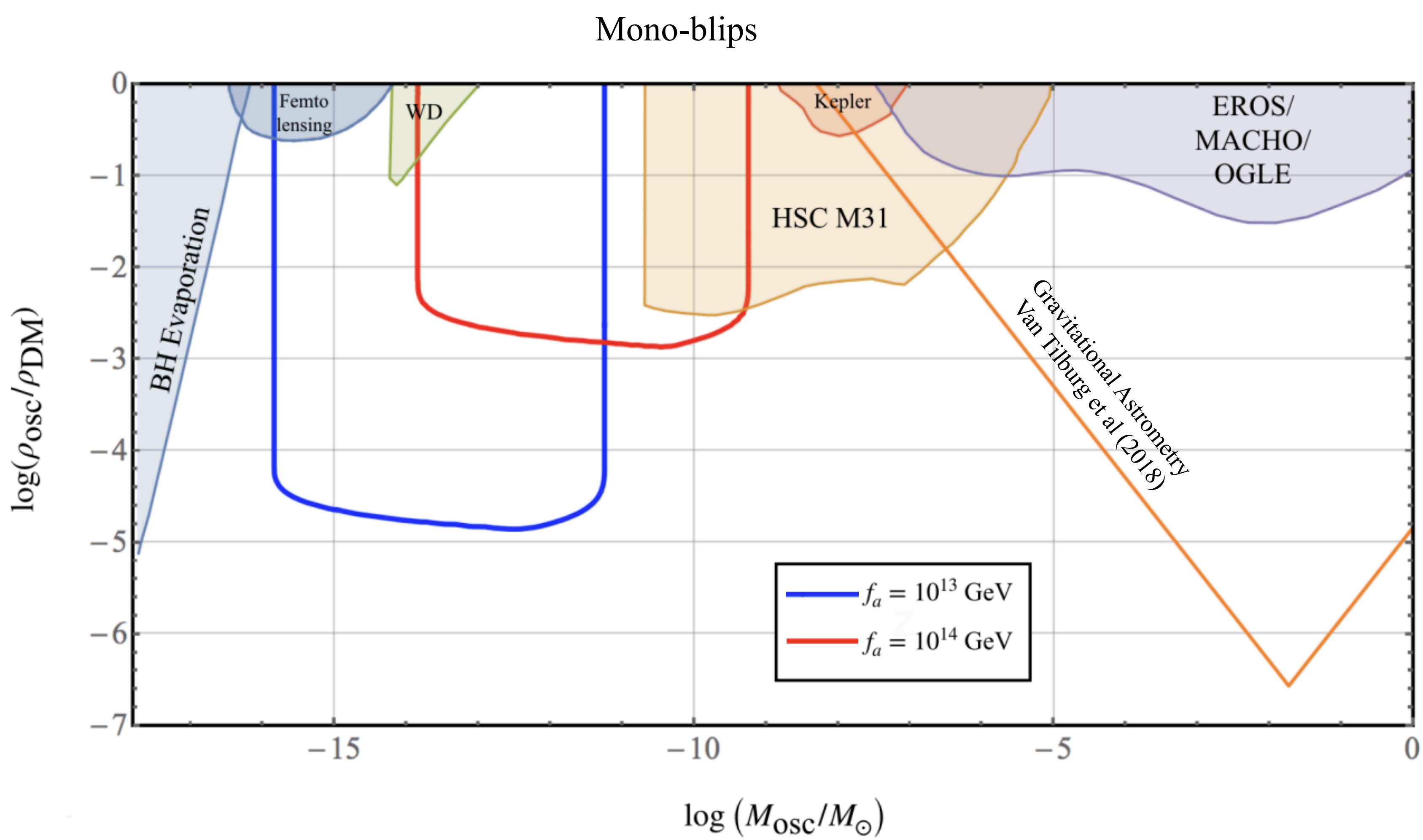

Overview

I. Axions as DM Candidates

II. Formation of Axion Clumps

III. Non-gravitational Lensing Effects of Axion Clumps

IV. Resonant Conversion of Axion Clumps Around NSs.

V. Summary & Conclusions

Axion-Photon Coupling

$$\boxed{\mathscr{L} \supset -\frac{g_{a\gamma\gamma}}{4} a\tilde{F}^{\mu\nu}F_{\mu\nu} = -\, g_{a\gamma\gamma} a\mathbf{E}\cdot\mathbf{B}}$$

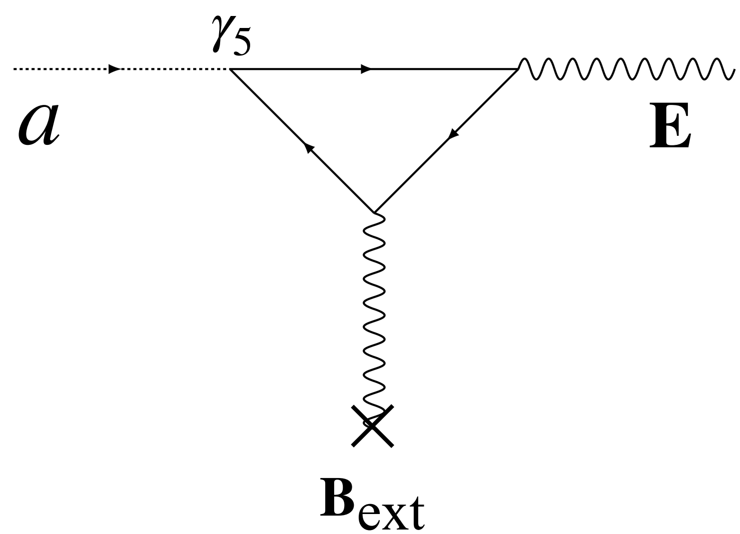

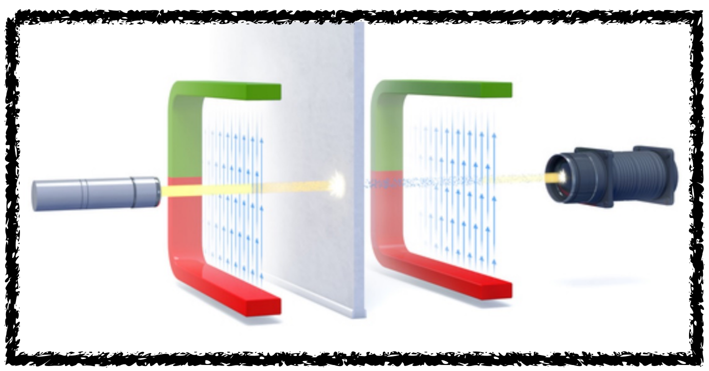

Light Shining Through Walls

Figure: DESY

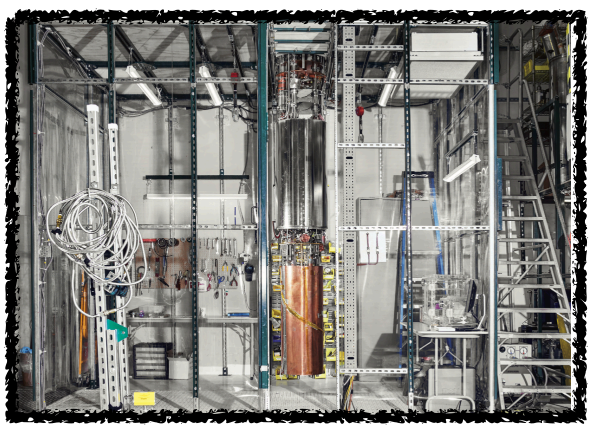

ADMX

Figure: Scientific American

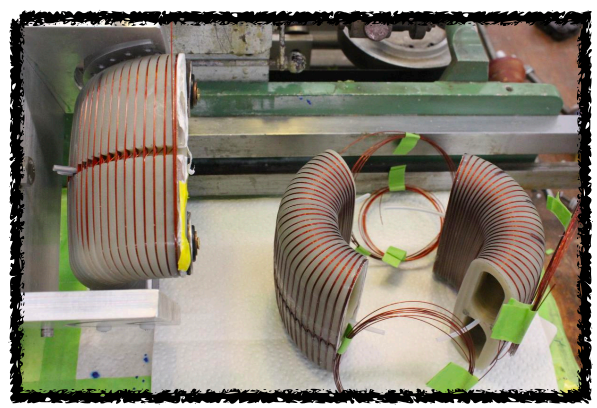

ABRACADABRA

Kahn, Safdi, Thaler (2016)

AS-NS Collisions

Axion Miniclusters
Tkachev (2014)

Solitons
Iwazaki (2014)

Fast Radio Bursts?

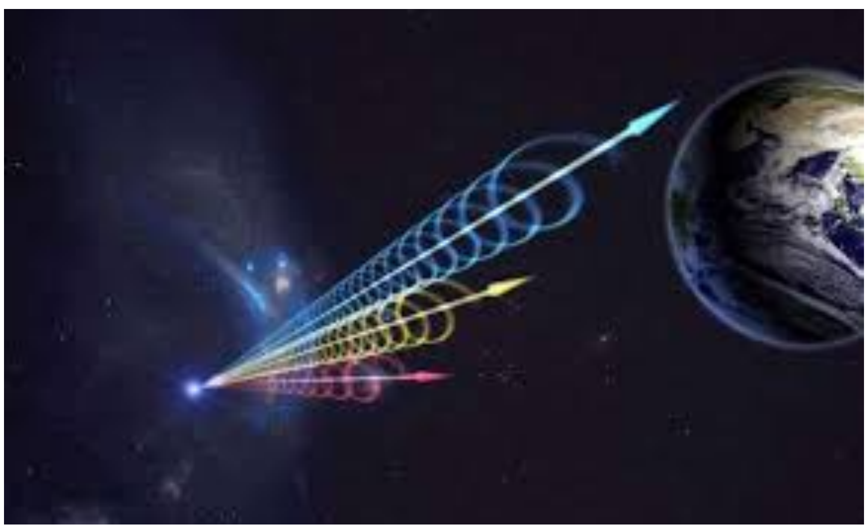

Credit: Jingchuan Yu, Beijing Planetarium/NRAO

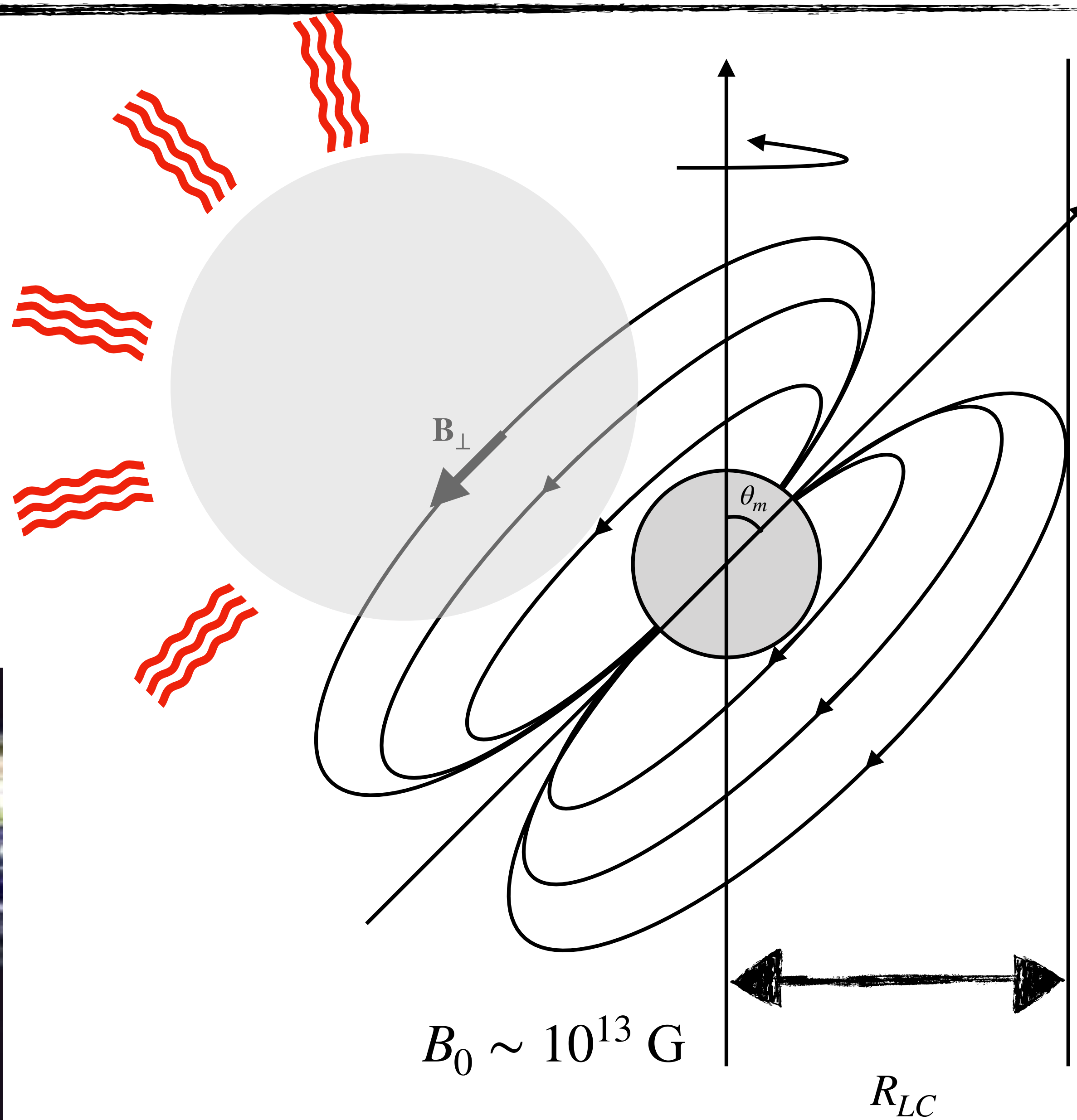

Non-Resonant Conversion

Axion-Photon Conversion

$$\mathscr{L} = g_{a\gamma\gamma} a \mathbf{E} \cdot \mathbf{B}_{ext}$$

CAST: Wikipedia

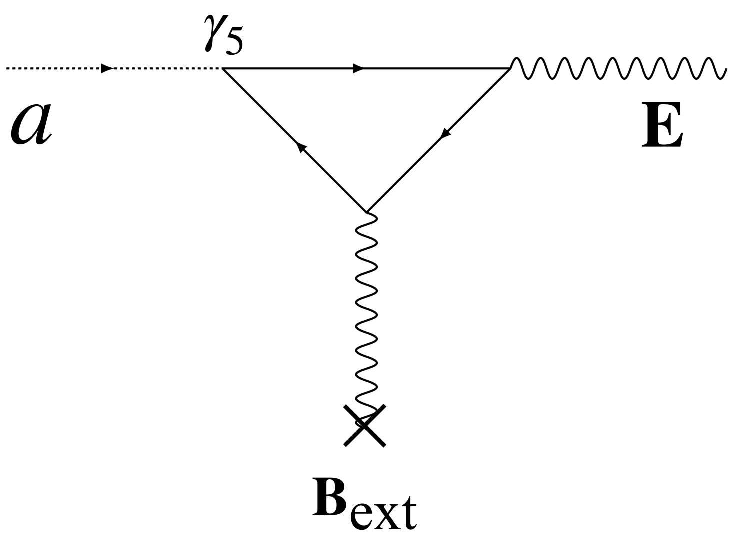

$$m_a = \omega, \quad p_a \neq p_\gamma$$

Non-resonant Conversion

$$P_{a\to\gamma} = \left(g_{a\gamma\gamma} |\mathbf{B}_{ext}| L \right)^2 \qquad \begin{cases} L_{app} & \Delta k L_{app} \ll 1 \\ \dfrac{\omega}{m_a^2} & \Delta k L_{app} \gg 1 \end{cases}$$

Resonant Conversion

Raffelt, Stodolsky (1988)
Hook, Kahn, Safdi, Sun (2018)

- Pulsars possess large $\vec{B}$-fields and a spatially varying plasma density.

Goldreich-Julian Model

$$\omega_p(r) \sim 20\ \mu\text{eV} \left(\frac{B_0}{10^{13}\ \text{G}}\right)^{1/2} \left(\frac{r}{r_{NS}}\right)^{-3/2}$$

- At some ``critical'' radius r_c, $\omega_p(r_c) = m_a$ and axions may resonantly convert to photons.

$$P_{a\to\gamma} \approx g_{a\gamma\gamma}^2 B(r_c)^2 L_{eff}^2 \qquad L_{eff} = \sqrt{\frac{r_c}{m_a}}$$

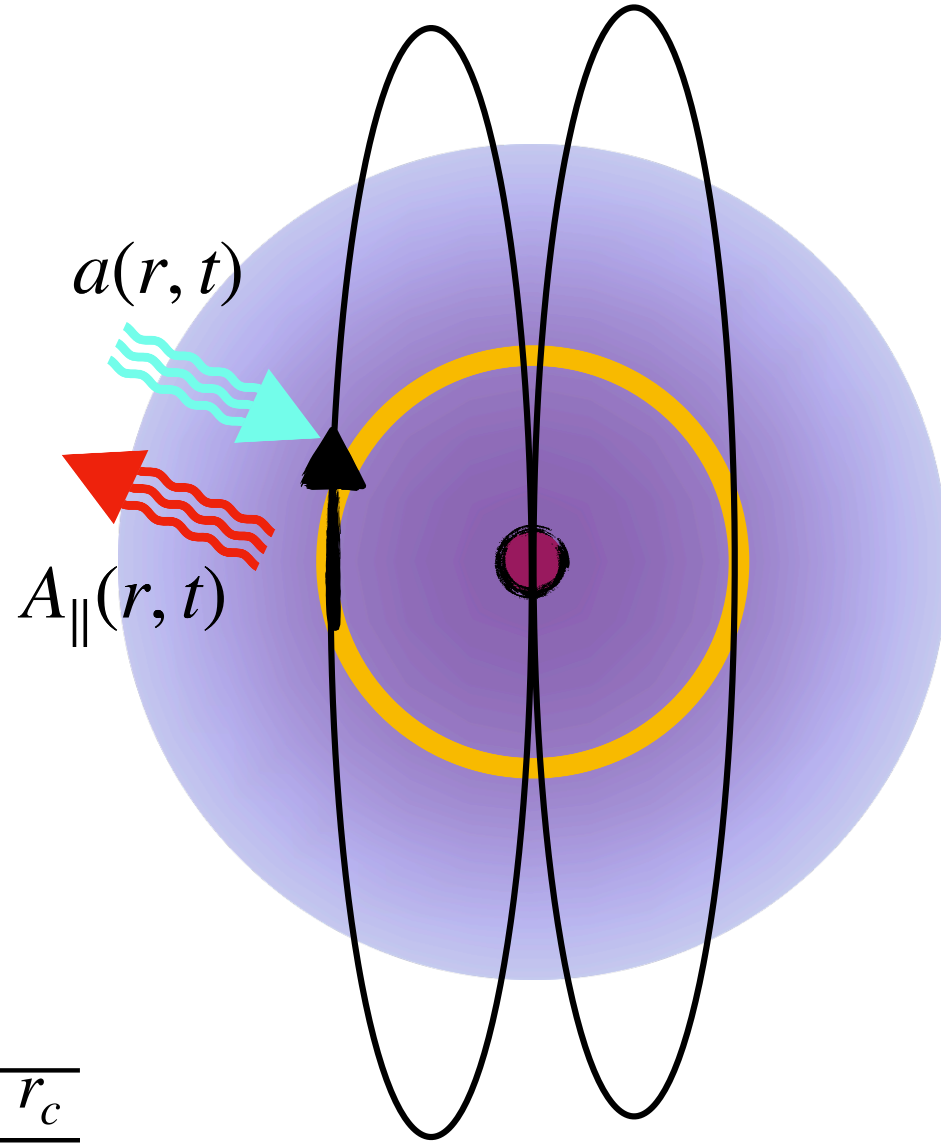

Resonant Conversion of Oscillons

- In order for resonant conversion to take place, the axion star much remain tidally stable until it reaches r_c.

Resonant Conversion of Oscillons

- In order for resonant conversion to take place, the axion star much remain tidally stable until it reaches r_c.

Femtohalo	Minicluster	Soliton	Oscillon
✗	✗	✗*	✓

Resonant Conversion of Oscillons

- In order for resonant conversion to take place, the axion star much remain tidally stable until it reaches r_c.

Femtohalo	Minicluster	Soliton	Oscillon
✗	✗	✗*	✓

$$\Phi = \frac{P}{4\pi d^2 (m_a/2\pi)} = 8.2 \times 10^4 \text{ Jy} \left(\frac{B_0}{10^{14}\text{ G}}\right)^{1/6} \left(\frac{m_a}{10^{-6}\text{ eV}}\right)^{5/3} \left(\frac{d}{1\text{ kpc}}\right)^{-2}$$

$$\Gamma_{\rm GC} \approx 200\text{ yr}^{-1} \left(\frac{m_a}{10^{-6}\text{ eV}}\right)^{1/3} \left(\frac{f_a}{10^{12}\text{ GeV}}\right)^{-2} \left(\frac{B_0}{10^{14}\text{ G}}\right)^{1/3} \left(\frac{N_{\rm bulge}}{6\times 10^8}\right) \left(\frac{P}{1\text{ sec}}\right)^{-1/3}$$

Flux of Sun on Earth: $\Phi = 1.6 \times 10^6$ Jy (at 1.4 GHz)

Projected Sensitivity

- Observation of the GC ($T = 1$ year), with current and planned radio telescopes, optimized for field-of-view.

$$g_{a\gamma\gamma} = \alpha/(2\pi f_a),\ P_{NS} = 1\ \text{sec},\ B_0 = 10^{13}\ \text{Gauss}$$

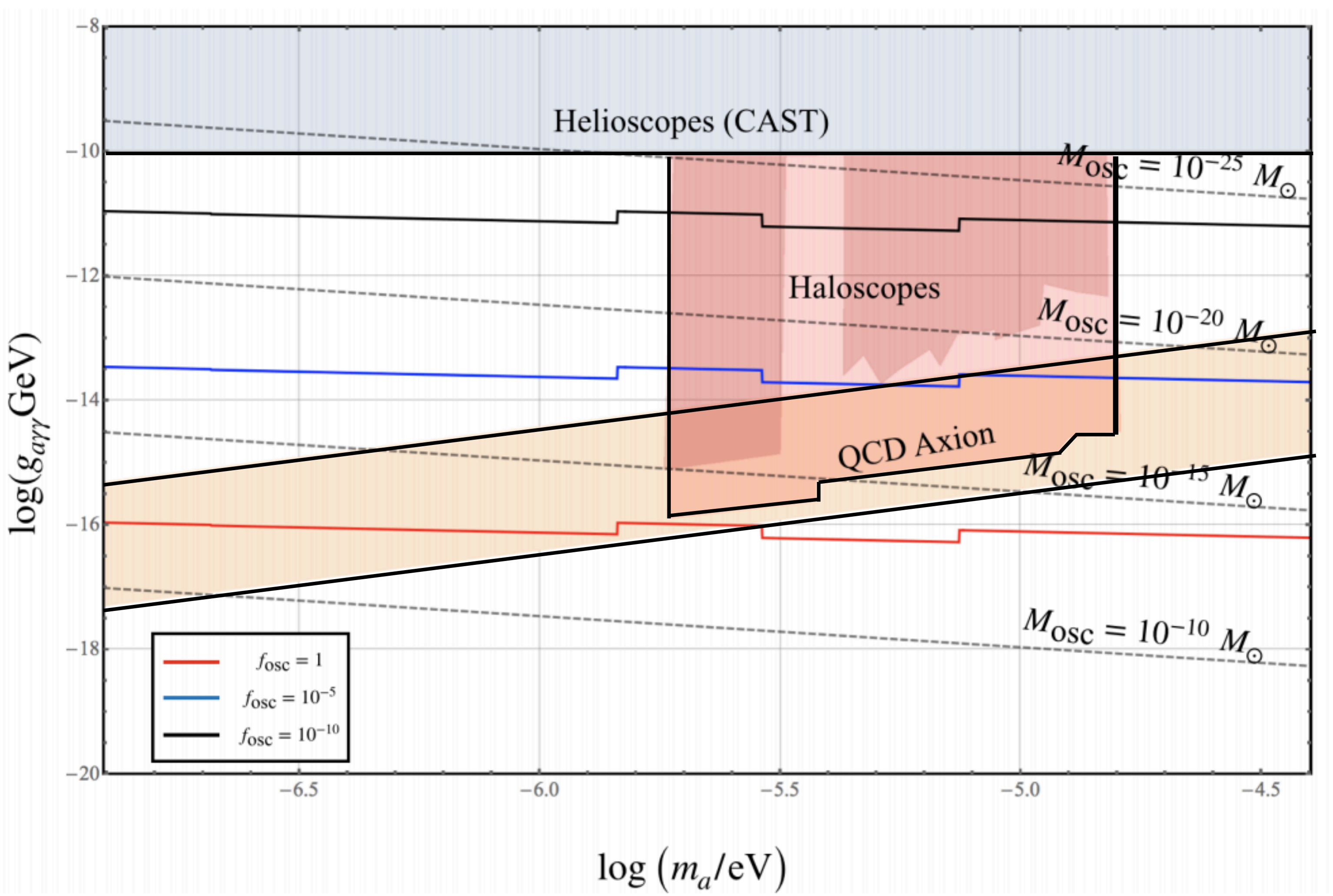

Outlook

So FRBs?

- Many axion clumps will be tidally destroyed before converting significantly (still potentially detectable EM signatures).
- Oscillons are the most promising candidate among axion clumps.
- FRBs have been observed over a range of frequencies ~ 328 MHz $- \ 8$ GHz . Cannot be explained by a single axion.

Summary

- Several cosmological scenarios lead to the formation of dense axion clumps
- These clumps may be detected by their non-gravitational lensing signature or by photons produced when they collide with NSs.
- Collisions with NSs may be responsible for some FRBs.
- Electromagnetic signatures may reach parameter space inaccessible to gravitational searches.

Thank you for your attention!

Questions?

Supplemental Slides

Plasma Lensing

- Degeneracy with plasma inhomogeneities?

$$\boxed{n_p(\mathbf{r}) = 1 - \frac{\omega_p^2(\mathbf{r})}{\omega^2}} \qquad \text{c.t.} \qquad \boxed{n_a(\mathbf{r}) = 1 - \frac{g_{a\gamma\gamma}^2 \dot{a}(\mathbf{r},t)^2}{16\omega^2}}$$

- Time dependence of axion field imprints spectral distortions at frequency $2m_a$.

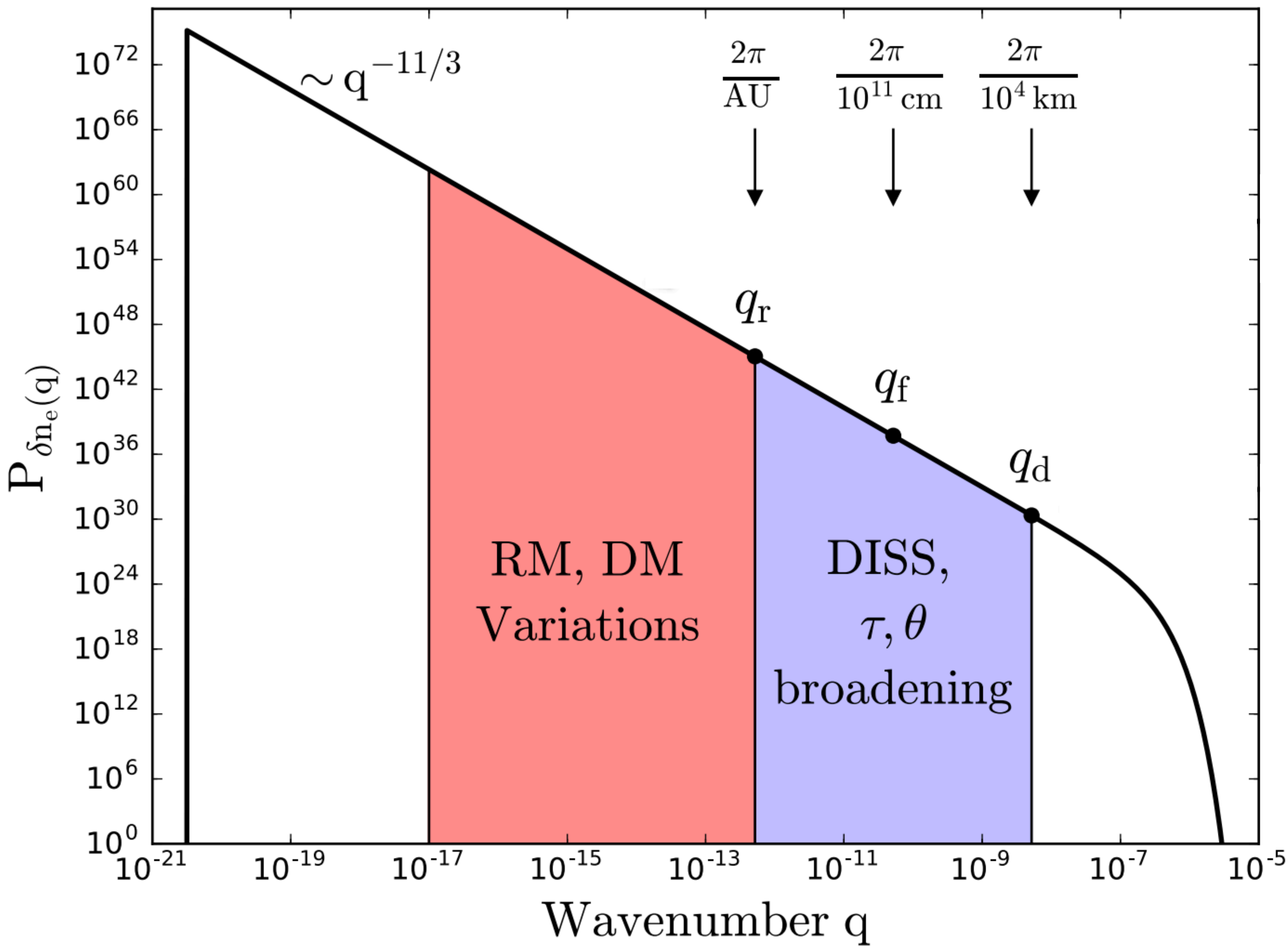

$\sim q^{-11/3}$
$\frac{2\pi}{\mathrm{AU}}$
$\frac{2\pi}{10^{11}\,\mathrm{cm}}$
$\frac{2\pi}{10^{4}\,\mathrm{km}}$
q_r
q_f
q_d
RM, DM Variations
DISS, τ, θ broadening
$P_{\delta n_e}(q)$
Wavenumber q
10^{0} 10^{6} 10^{12} 10^{18} 10^{24} 10^{30} 10^{36} 10^{42} 10^{48} 10^{54} 10^{60} 10^{66} 10^{72}
10^{-21} 10^{-19} 10^{-17} 10^{-15} 10^{-13} 10^{-11} 10^{-9} 10^{-7} 10^{-5}

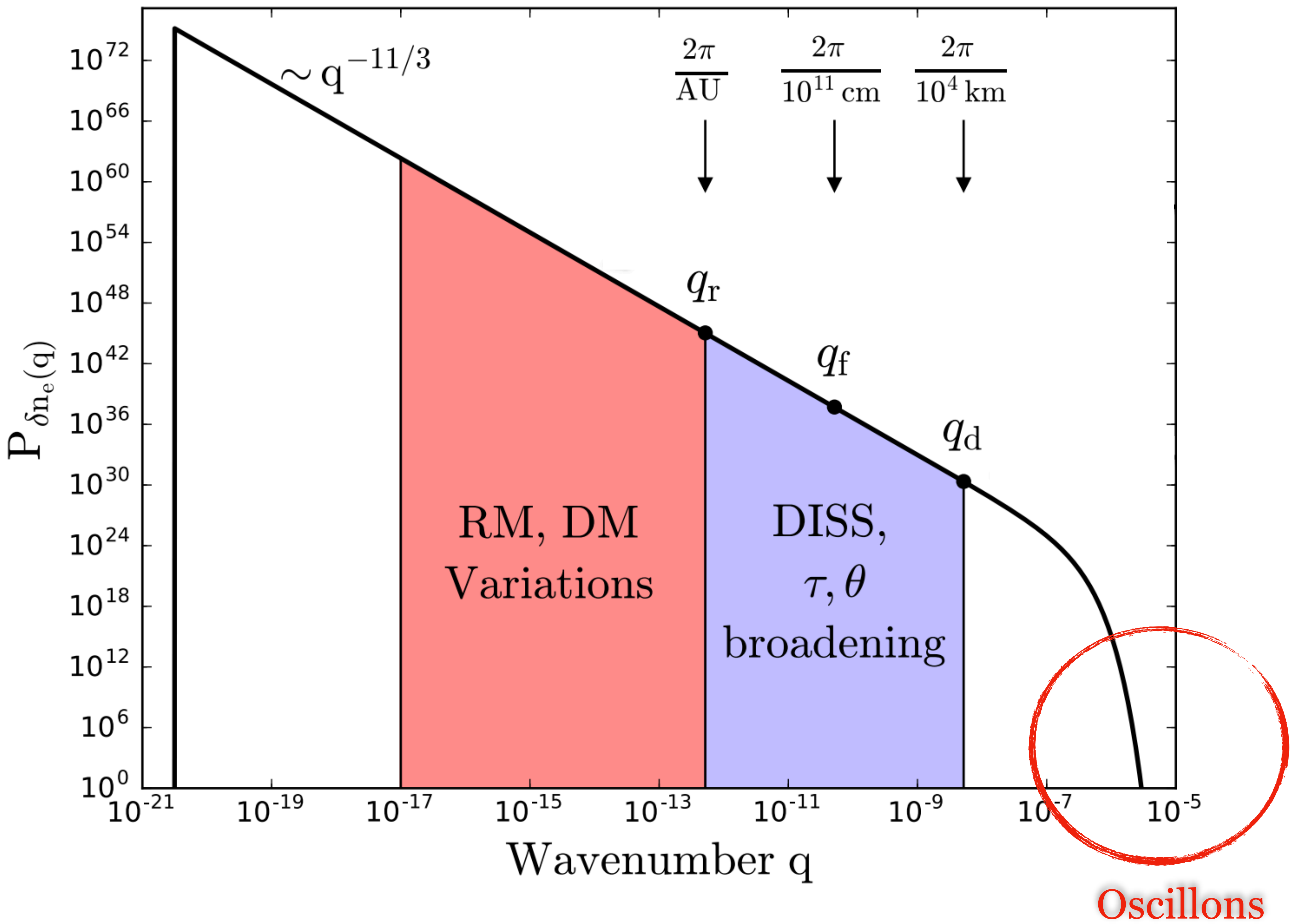

$P_{\delta n_e}(q)$
10^{72}
10^{66}
10^{60}
10^{54}
10^{48}
10^{42}
10^{36}
10^{30}
10^{24}
10^{18}
10^{12}
10^{6}
10^{0}
$\sim q^{-11/3}$
$\frac{2\pi}{\mathrm{AU}}$
$\frac{2\pi}{10^{11}\,\mathrm{cm}}$
$\frac{2\pi}{10^{4}\,\mathrm{km}}$
q_r
q_f
q_d
RM, DM Variations
DISS, τ, θ broadening
10^{-21}
10^{-19}
10^{-17}
10^{-15}
10^{-13}
10^{-11}
10^{-9}
10^{-7}
10^{-5}
Wavenumber q
Oscillons